Journal of African Earth Sciences 56 (2010) 59–74

Contents lists available at ScienceDirect

Journal of African Earth Sciences

journal homepage: www.elsevier.com/locate/jafrearsci

Quaternary extrusive calciocarbonatite volcanism on Brava Island (Cape Verde): A nephelinite-carbonatite immiscibility product

Cyntia Mourão [a,b,*], João Mata [a,b], Régis Doucelance [c], José Madeira [a,d,e], António Brum da Silveira [a,d,e], Luís C. Silva [b,f], Manuel Moreira [g]

[a] Faculdade de Ciências da Universidade de Lisboa, Departamento de Geologia (GeoFCUL), Campo Grande, C6, 1749-016 Lisboa, Portugal
[b] Centro de Geologia da Universidade de Lisboa (CeGUL), Campo Grande, C6, 1749-016 Lisboa, Portugal
[c] Laboratoire Magmas et Volcans (UMR 6524 CNRS), Observatoire de Physique du Globe de Clermont-Ferrand, Université Blaise Pascal, 5 rue Kessler, 63038 Clermont-Ferrand Cedex, France
[d] LATTEX – Laboratório de Tectonofísica e Tectónica Experimental, 1749-016 Lisboa, Portugal
[e] IDL – Instituto D. Luís, 1250-102 Lisboa, Portugal
[f] Instituto de Investigação Científica e Tropical, 1300-344 Lisboa, Portugal
[g] Laboratoire de Géochimie et Cosmochimie (UMR 7579 CNRS), Institut de Physique du Globe de Paris, Université Paris 7, 4 Place Jussieu, 75252 Paris Cedex, France

ARTICLE INFO

Article history:
Received 3 October 2008
Received in revised form 29 May 2009
Accepted 9 June 2009
Available online 14 June 2009

Keywords:
Extrusive carbonatite
Brava Island
Cape Verde
Sr–Nd isotopes
Immiscibility

ABSTRACT

The Cape Verde volcanic archipelago, located in the oceanic portion of the African plate some 500 km west of the Senegal coast, is renowned for the occurrence of carbonatites on at least 5 of its 10 islands. In this study we report the occurrence of about twenty new small outcrops of extrusive carbonatites on Brava Island (64 km^2), the south-westernmost island of the archipelago. These new occurrences are studied from geological, petrographic, mineral chemistry and whole rock (elemental and isotopic) geochemical points of view, allowing for a discussion of their petrogenesis and emphasising their geological and geochemical peculiarities in the context of the Cape Verde carbonatites.

Most of the extrusive carbonatitic formations correspond to pyroclastic rocks, comprising magmatic and/or phreatomagmatic ash and lapilli fall deposits and one probable pyroclastic flow. Lava flows occur at one locality. The predominance of pyroclastic facies demonstrates the significant explosivity of these magmas characterised by very low viscosity. Independent of the modes of emplacement, all samples are calciocarbonatites and exhibit a remarkable compositional uniformity, considering that they represent several different eruptions and present a wide geographical dispersion.

Brava extrusive carbonatites belong to the younger (probable Holocene – Pleistocene) volcanic sequence of the island. This feature is unique in the context of Cape Verde geology, because in the other islands (including Brava) of the archipelago carbonatites are commonly assigned to the basal complexes, having formed during a fairly early stage of the emerged evolution of volcanic construction.

Compared with the older intrusive sövitic rocks occurring at Middle Unit of Brava Island, extrusive facies are more iron and manganese rich and yield higher contents of trace elements like Ba, Th, U, Nb, Pb and REE, but somewhat lower Sr abundances. New initial Sr and Nd isotope data (0.703557–0.703595 and 0.512792–0.512816, respectively) determined in extrusive calciocarbonatitic rocks are clearly different from those obtained in intrusive rocks (0.703340–0.703356 and 0.512910–0.512912, respectively), which demonstrates that the studied rocks were ultimately the product of a source distinct from those that produced the older intrusive carbonatites. Brava extrusive carbonatites yield isotope signatures that are clearly distinct from all other Cape Verde carbonatites, but akin to the Southern Cape Verde silicate rocks. We propose that the extrusive carbonatites resulted from an immiscibility process that also produced conjugate melts of nephelinitic composition.

1. Introduction

Carbonatites are igneous rocks containing more than 50% by volume of carbonate minerals. Intrusive facies clearly dominate over extrusive ones, which represent only ≈10% of the known occurrences worldwide (Woolley and Church, 2005).

Despite the fact that carbonatite–oceanic mantle interactions have been shown to occur in some areas (e.g., Polynesia: Hauri

* Corresponding author. Address: Faculdade de Ciências da Universidade de Lisboa, Departamento de Geologia (GeoFCUL), Campo Grande, C6, 1749-016 Lisboa, Portugal.
E-mail address: ccmourao@fc.ul.pt (C. Mourão).

1464-343X/$ - see front matter © 2009 Elsevier Ltd. All rights reserved.
doi:10.1016/j.jafrearsci.2009.06.003

et al., 1993; Chauvel et al., 1997; Grande Comore: Coltorti et al., 1999; Madeira: Mata et al., 1999; Kerguelen: Mattielli et al., 2002; Cape Verde: Martins et al., 2007), exposures of oceanic carbonatites are extremely rare and have been identified so far only in the Cape Verde archipelago (e.g., Assunção et al., 1965; Alves et al., 1979; Silva et al., 1981; Kogarko, 1993) and the Canary Islands (e.g., Fúster et al., 1968; Allègre et al., 1971), both located on the African plate (see also Hoernle et al., 2002). In the Canary archipelago, carbonatites are represented only by intrusive calciocarbonatites within the basal complex of Fuerteventura (e.g., Muñoz et al., 2005; De Ignacio et al., 2006). In the Cape Verde islands carbonatites occur on at least 5 of the 10 islands and on the islets near Brava (Aires-Barros, 1968; Machado et al., 1968; Fig. 1). They range in composition from calcio- to magnesiocarbonatites. In this archipelago, intrusive carbonatites are clearly dominant, despite an important volcanic occurrence described by Silva et al. (1981) on Santiago Island and those reported hereafter on Brava Island.

Assunção et al. (1965) were the first authors to coin the term "carbonatites" to describe carbonate rocks considered of igneous origin on Brava. Subsequently, Machado et al. (1968) mapped several outcrops of intrusive carbonatites within the basal complex (see also Madeira et al., 2006). The first mention of Brava extrusive carbonatites was made in an abstract (Peterson et al., 1989). More recently, Hoernle et al. (2002) briefly mentioned an occurrence of carbonatite lava flows on Brava Island related to a small cone at Cachaço, on the central part of the island, to which they assigned a very recent age (<1000 years) based on its non-eroded morphology. They also offered a petrographic description with the element and isotopic compositions of one sample. During two field campaigns in 2006 and 2007, we discovered several (≈20) new outcrops of volcanic carbonatites corresponding to at least five distinct eruptions (Fig. 1).

Compared with their intrusive counterparts, extrusive carbonatites are usually considered more probably representative of the pristine compositions of carbonatite magmas (e.g., Bailey, 1993; Woolley and Church, 2005). Given the recognised importance of extrusive carbonatites to the understanding of the petrogenesis of these non-silicate magmas, we describe in this paper the newly discovered occurrences on Brava from geological, petrographic and whole rock (elemental and isotopic) geochemical points of view. This allows us to (1) discuss the petrogenesis of the extrusive carbonatites; (2) determine whether they are ultimately derived from the source that previously delivered the intrusive carbonatites from the Middle Unit; (3) compare their geochemical characteristics with those reported for the other Cape Verde carbonatites; and (4) emphasise the uniqueness of the Brava extrusive carbonatitic rocks in the context of Cape Verde volcano-stratigraphy.

2. Geology

The Cape Verde Archipelago consists of 10 major islands and several islets (Fig. 1), arranged in a westward open "horseshoe" emplaced on a 2.2 km-high and 1200 km-wide topographic "swell" (Cape Verde Rise). This swell correlates with geoid and gravimetric anomalies (Monnereau and Cazenave, 1990), and is considered the result of the impingement of lithosphere by a deeply anchored mantle plume (e.g., Montelli et al., 2006), with resulting plate thinning and heating.

Brava is a small island (64 km^2) located on the south-western tip of the approximately NE–SW alignment formed by the Southern Cape Verde islands (Fig. 1). Three major volcano-stratigraphic units are identified (Fig. 1B; Madeira et al., 2006). The older Lower Unit is composed of an uplifted nephelinite/ankaratrite submarine volcanic sequence that includes pillow lavas, pillow breccias and hyaloclastites. This represents the upper part of the submarine seamount precursor of the island. A subvolcanic plutonic complex intrudes the Lower Unit and includes syenites, pyroxenites, ijolites and carbonatites. This Middle Unit corresponds to magma chambers related to a volcanic phase that is no longer preserved in the geologic record.

The younger volcanic sequence, forming the Upper Unit, rests on an important erosional discontinuity truncating the older basement (Lower and Middle units). This sequence is dominated by products of phonolite volcanism characterised by phreatomagmatic and phreatoplinian eruptions and by the extrusion of domes and lava flows. Rare mafic products, predominantly of nephelinitic composition, are also present and include a phreatomagmatic crater, a strombolian cone and a few scattered small-volume lava flows. Although no eruptions have occurred since settlement in the mid-XVth century, the fresh morphology of craters and domes indicates that volcanism must be considered active. This fact, together with the occurrence of fault scarps, frequent seismicity, and strong relief, indicates a significant risk to the population of Brava related to volcanic, seismo-tectonic, mass movement and tsunami hazards. On Brava major mass movements occur in relation to steep slopes of erosive (sea cliffs and fluvial valleys) or structural nature (Madeira et al., 2009).

Extrusive carbonatites (Fig. 1B) exposed within the Upper Unit constitute the main aim of this contribution. During field works in 2006 and 2007, at least 20 small outcrops of dark-brown to blackish extrusive carbonatites were found, none of which corresponds to the location described by Hoernle et al. (2002). These occur in three areas: NE of the island, around Nova Sintra (Fig. 1B and C), SW near Campo Baixo (Fig. 1B and D), and S around Cachaço and Morro das Pedras (Fig. 1B and E). All extrusive carbonatites were deposited on or near the top of the younger volcanic sequence.

Unlike the description of Hoernle et al. (2002), most outcrops are made up of pyroclastic formations, comprising magmatic and/or phreatomagmatic ash and lapilli fall deposits and one probable pyroclastic flow, and most contain abundant lithic fragments of phonolite and occasionally other lithologies. Lava (alvikite) flows may also be present in the Santa Bárbara outcrop.

Near Nova Sintra village, extrusive carbonatites crop out in two locations (Fig. 1B and C). One is located 300 m to the north of Santa Bárbara where carbonatite ash (Fig. 4a) partially fills a wide and shallow crater carved into the NE slope of the island, forming a small step in the morphology. Just outside the volcanic depression, carbonatite deposits display a massive texture and may correspond to the remains of lavas that flowed towards the eastern shore (Fig. 4b). Stratigraphically, these deposits are the youngest in the area, covering all other formations and cropping out on the topographic surface.

On the road to Mato Grande, 750 m SW of the centre of Nova Sintra village (Fig. 1B and C), the road-cut exposes a carbonatite pyroclastic fall deposit intercalated between phonolitic phreatomagmatic pyroclasts and a phonolitic pumice fall deposit (Fig. 2A). The deposit is composed of fine stratified ash containing mica crystals and small phonolite lithic fragments. It was displaced by N–S-trending normal faults and is truncated by an erosional surface. To the NW, carbonatite tuffites, containing terrestrial gastropods, represent sedimentary removal of the volcanic carbonatite ashes. Grain-size analysis of the deposit shows that it is mostly composed of fine to very fine-ash and dust ($\sim$95 wt.% < -1 Φ). The coarser fraction contains lithic fragments of phonolite from the Upper Unit, and pyroxenite and sövite from the Middle Unit. This is the oldest of the observed extrusive carbonatite deposits.

The outcrops SW of Campo Baixo (Figs. 1B and D, 2B) include pyroclastic fall deposits, a feeder dike (Fig. 3a) and the remains of a small hornito or spatter rampart (Fig. 3b). In cross section, the deposit is composed of layers of vesicular lapilli (5–10 mm in

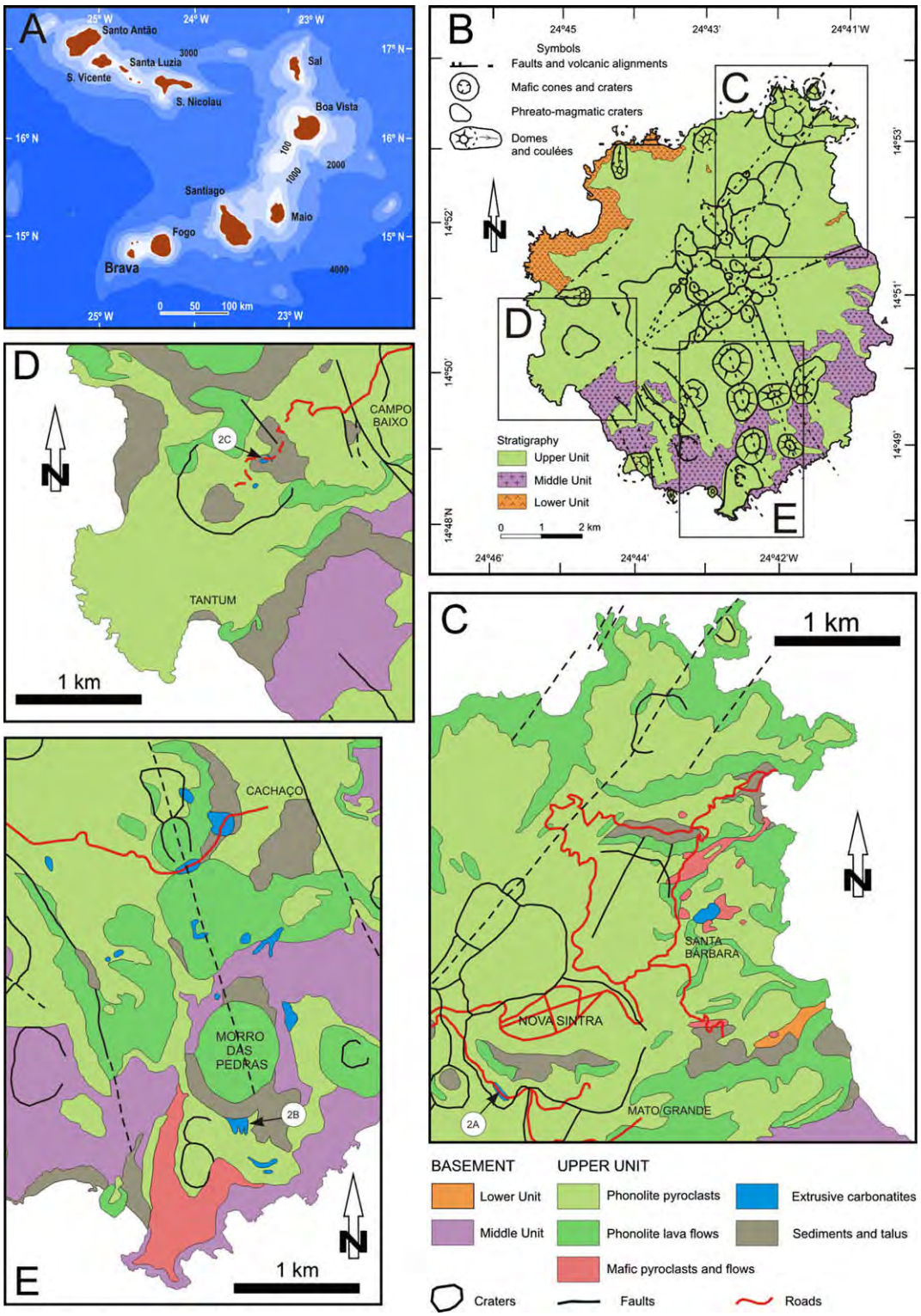

Fig. 1. Geology of Brava Island. (A) Location of Brava in the Cape Verde archipelago, (B) simplified geological map of Brava representing the main stratigraphic units and structures. Rectangles (C), (D), and (E) correspond to areas shown below in more detailed geologic maps. Orange and lilac colours represent the older basement (Lower and Middle Units). In the Upper Unit, blue areas correspond to the mapped extrusive carbonatite outcrops. The locations of geological sections from Fig. 2 are marked with labels 2A, 2B and 2C. Localities cited in the text are indicated.

diameter; Fig. 3c) and a crystal-rich tuff (Fig. 3d). The pyroclasts are preserved in two small outcrops blanketing a few tens of square metres of the present topography, one of which can be linked to the feeder dike, whereas the second lies 250 m from the eruptive centre. The NW–SE-trending 1 m-thick conduit displays a fragmented (pyroclastic) texture in the centre and massive chilled margins (Fig. 4c and d). It contains abundant lithic fragments of variable size (Fig. 3a). A small hornito or spatter rampart is constructed above the dike, forming a small mound on the topography (Fig. 3b). These deposits represent the youngest

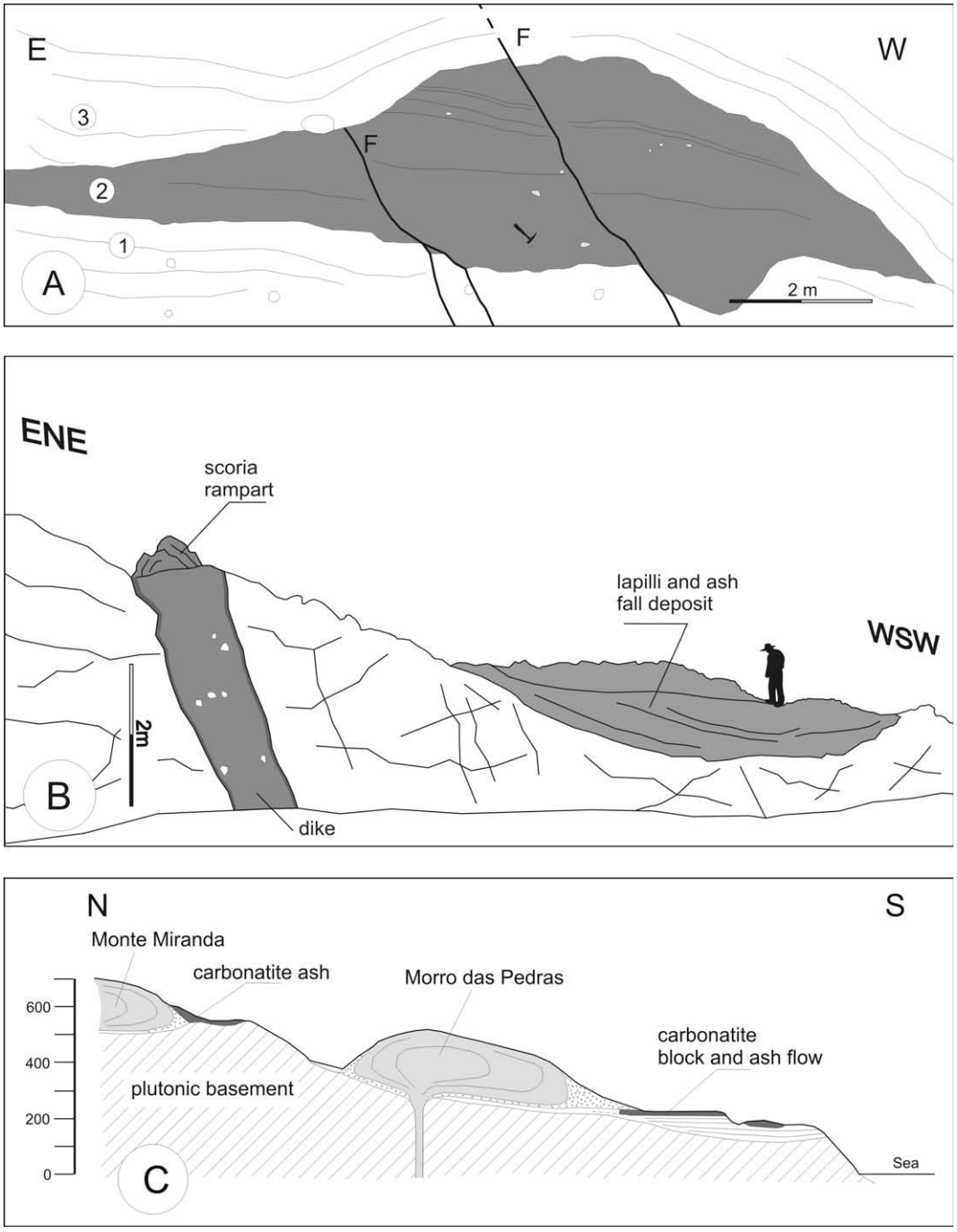

Fig. 2. Field sketches of recent extrusive carbonatites (in dark-grey); locations indicated in Fig. 1 C–E. (A) Section on the road to Mato Grande: carbonatitic fine-ash deposit overlies a phonolitic phreatomagmatic tuff and is covered by a coarse phonolitic pumice fall deposit. Erosion truncated the carbonatite deposit prior to the pumice fall event. The deposits are displaced by two surface ruptures along N-S-trending faults, (B) exposure along the road to Tantum exposing a carbonatitic dike, the remains of a spatter rampart, and a lapilli and ash-fall deposit. Note the presence of chilled margins (darker) and lithic fragments in the dike. The view is oblique and the scale (given by the vertical bar and figure in the background) is variable. Details of this outcrop are displayed in the photos in Fig. 3a–c and d, and (C) stratigraphic relations and location of the carbonatite deposits surrounding the Morro das Pedras phonolite dome. Carbonatitic block and ash-flow deposit is located south of the dome and partially covered by it. To the north, in higher topographic positions, there are several outcrops of a carbonatite ash-fall deposit, probably belonging to the same eruptive event. The vent of the carbonatitic eruption must be concealed by the younger dome. Photos of the block and ash-flow are presented in Fig. 3e and f.

volcanic event in the area, because they are stratigraphically above all others.

The outcrops south of Morro das Pedras (Figs. 1B and E, 2C) correspond to a flow deposit, probably a block and ash-flow. The deposit flowed down a wide, shallow valley and presents variable thickness (7 m-thick in the centre, thinning laterally) and a flat top (Fig. 3e). It is composed of a slightly consolidated carbonatite ash matrix supporting abundant lithic fragments, exclusively of phonolite composition. Bigger clasts, ranging in size from 40 cm up to 3 m in diameter, are rounded (but not polished) and covered by a thin, dark-grey film of massive carbonatite, probably formed by agglutinated and partially welded ash (Figs. 3f, 4e). In contrast, smaller fragments are angular, suggesting that bigger lithic fragments suffered abrasion during transport, whereas smaller clasts were immersed in ashes and preserved from abrasion. This was the penultimate event in the region, predating the formation of

Fig. 3. Field photographs of three outcrops of the recent extrusive carbonatites of Brava Island. (a) Carbonatite dike, 1 m-wide, exposed along the road to Tantum. The dike crosscuts a highly fractured landslide deposit of phonolitic nature. The walking stick to the left of dike is 1.10 m-long, (b) remains of carbonatite spatter rampart standing on the topographic surface above the feeder dike. Hammer for scale, (c) and (d) details of carbonatite lapilli fall deposits at outcrop along the road to Tantum. Pen point is 1 mm wide: vesicular carbonatite lapilli-fall layer (c); crystal-tuff layer formed by accumulation of 1 mm-thick, 2–3 mm-long tabular calcite crystals (d), (e) general view of the carbonatitic block and ash-flow of the Morro das Pedras area, looking north. The carbonatite is the darker deposit on which the human figure (circled) stands. The carbonatites rest on phonolitic phreatomagmatic tuffs. The very young phonolite dome and related breccia overlie the carbonatite, (f) detail of a phonolite block rounded by abrasion within the carbonatitic block and ash-flow from the same locality and (g) small outcrop of spatter accumulation in the Cachaço area, indicating proximity to the eruptive centre. Hammer for scale.

the impressive phonolite dome of Morro das Pedras (250 m in height), which presents an almost untouched volcanic morphology (Fig. 3e). To the north and west of the dome, several small outcrops of carbonatite ash may correspond to pyroclastic fall deposits related to the same eruption. The position of the carbonatitic fall and flow deposits suggests that the eruptive centre for this event may have been covered by the Morro das Pedras dome. Fall deposits were blown to the N and NW of the eruptive centre, whereas ash flows followed the fluvial valley downwards to the south.

A few more outcrops of carbonatite are located to the NW, W and SW of the village of Cachaço (Fig. 1B and E). Most appear to represent consolidated lapilli and ash deposits (Fig. 4f), yielding some solution (corrosion) morphologies. The eruptive centre for these deposits must be placed on the SE slope of the Cachaço phonolite dome, where the carbonatite outcrops display a granular texture that may represent accumulations of agglutinated coarse lapilli and spatter, suggesting proximity to the volcanic source (Fig. 3g). All other deposits lie to the west of this location, indicating easterly winds during this event. Carbonatitic pyroclasts overlie all other volcanic deposits in the area, indicating a very recent age for the event.

The described stratigraphic and structural relations, as well as the geographic distribution of the extrusive carbonatites, points to at least five distinct, very recent carbonatitic eruptions. The

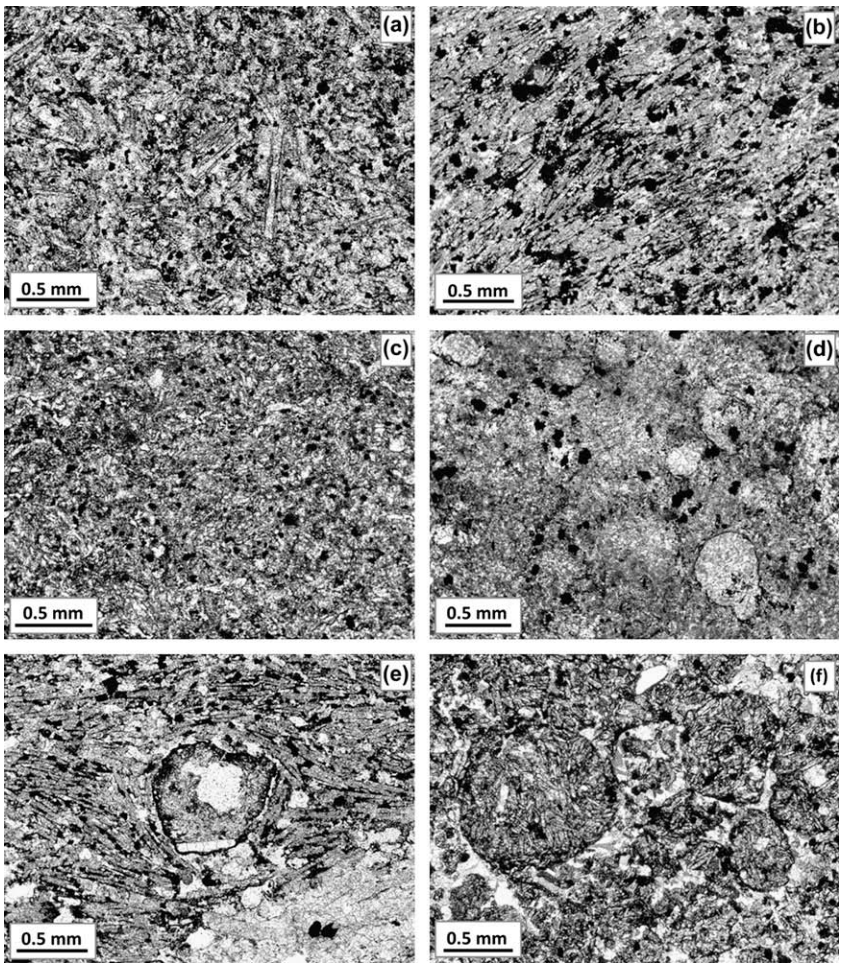

Fig. 4. Photomicrographs of representative extrusive carbonatites of Brava Island. (a) Tabular calcite phenocrysts with random orientations supported by very fine-grained ash matrix (sample CY-219) in the Santa Bárbara carbonatite outcrop, (b) well-developed trachytic-like texture of a lava flow, produced by oriented tabular calcite crystals in the same locality (sample CY-222), (c) and (d) aspects of the chilled margin of the carbonatite dike exposed on the road to Tantum; (c) is a very fine-grained carbonatite, whereas thin section (d) of the inner edge of the chilled margin shows a few spherical droplets of carbonatite in a fine-grained matrix (Sample CY-261), (e) tabular calcite crystals showing a well-developed flow orientation, from the film enveloping the phonolite blocks from the block and ash-flow deposit to the south of Morro das Pedras (sample CY-94) and (f) tear-drop ash-tuff cropping out to the SW of the village of Cachaço (sample CY-246). The deposit is composed of spherical ash particles with secondary spathic calcite filling interstitial voids.

older eruption must be the one that deposited the Mato Grande ash deposit, another is related to the Morro das Pedras event, the Cachaço deposits represent a third eruption, and the Santa Bárbara and Tantum outcrops probably represent the youngest (fourth and fifth) carbonatitic volcanic events.

3. Petrography

3.1. Extrusive carbonatites from the Upper Unit

According to the systematics of Woolley and Kempe (1989), all sampled outcrops of extrusive carbonatites are made up of calciocarbonatites.

Most pyroclastic deposits are ash-tuffs, with grains mostly smaller than 0.20 mm. Some consist of juvenile, tear-drop and spherical particles containing small tabular carbonate crystals without any preferential orientation, with the spaces between particles filled with secondary spathic calcite (Fig. 4f). Usually, pyroclastic particles are fine-grained and have ill-defined grain boundaries, which in some cases can result from a late re-crystallisation process. In a few samples, secondary spathic calcite cement is almost absent, and the rock is formed essentially by agglutinated, very fine carbonatite ash, with large tabular phenocrysts of calcite (Fig. 4a). These rocks are essentially composed of calcite, with apatite and biotite found in minor quantities. Alkali feldspar is very rare. Frequent accidental material, namely pyroxenite and phonolite, and coarse-grained calcite (from sövite) are present in the pyroclastic deposits, reflecting the lithological nature of the formations crossed by carbonatitic magma during its ascent.

Samples representing carbonatite lava flows (Fig. 4b) and agglutinated ash (Fig. 4e) show a marked flow orientation marked by the same kind of tabular carbonate crystals as in tuffs, creating a trachytic-like texture. The crystals are sub-angular laths with rounded edges, indicating the development of rhombohedral and pyramidal crystal faces. They often produce folded flow lines. The matrix, consisting of fine-grained calcite and oxide dust (magnetite?), is interpreted as resulting from quenching of the remaining carbonatite melt during eruption. Calcite is largely predominant, and apatite and biotite occur rarely.

3.2. Intrusive carbonatites from the Middle Unit

Intrusive calciocarbonatites occur only within the alkaline–carbonatite intrusive complex of the Middle Unit. They are here described for comparison with extrusive carbonatites.

Intrusive carbonatites tend to be equigranular, although some samples display a seriate texture. They are hypidiomorphic to allotriomorphic and are fine- to coarse-grained (0.02 mm–1.5 cm).

Two samples, however, show very large (>2 cm) carbonate crystals. Calcite, which is present in variable amounts, makes up the principal carbonate minerals in these rocks. Other constituents include apatite, alkaline feldspar and oxide minerals. Mica is lacking in many samples but, when present, can be fairly abundant (this mineral phase occurs in 5 of 14 samples). Sodic pyroxene, titanite, analcime and cancrinite are found as accessories.

4. Mineral chemistry

Selected EMP analyses of the main mineral phases of the pyroclastic deposits and lava flows are reported in Table 1, whereas Table 2 gives representative analyses of the most abundant minerals in the intrusive carbonatites from the Middle Unit for comparison.

4.1. Analytical procedures

The mineral compositions were determined at CeGUL/CREMINER (Faculdade de Ciências da Universidade de Lisboa) on a JEOL JXA 8200 microprobe, using a range of natural minerals as standards. An accelerating voltage of 15 kV was combined with a beam current of 10 nA and a beam diameter of 5 μm. Due to the low stability of some minerals under an electron beam and strong loss of Na, a defocused beam diameter (up to 20 μm) was sometimes used.

4.2. Results

The analysed apatites have very high F contents (>3.3 wt.%; > 0.88 atoms p.f.u.), even compared with those described in carbonatites worldwide (e.g., Seifert et al., 2000; Brassinnes et al., 2005; D'Orazio et al., 2007). They are, thus, fluorapatites. However, it should be emphasised that fluorapatite analyses from the studied extrusive carbonatites yielded F contents significantly above the stoichiometric value of 3.77 wt.% (up to 4.2 wt.% and 1.095 atoms p.f.u.). This is not very common but has been reported for some carbonatites (e.g., Bünh et al., 2001) and can be considered the result of coupled substitution involving the replacement of phosphorus by tetravalent carbon and of O^{2-} by F^{-} in order to maintain the charge balance: $[PO4]^{3-} \leftrightarrow [CO_3.F]^{3-}$;

Table 1
Representative EMP analyses (wt.%) of the major mineral phases of extrusive carbonatites.

Phase sample	Apatite			Calcite				Biotite			
	CY-95	CY-95	CY-95	CY-95	CY-95	CY-221	CY-221	CY-95	CY-95	CY-221	CY-221
	ap2	ap4	ap5	cb21	cb43	cb12	cb24	mc5	mc11	mc1	mc4
Major elements (wt.%)											
SiO_2	–	–	–	–	–	–	–	36.88	36.78	36.19	38.38
TiO_2	–	–	–	bdl	bdl	bdl	bdl	3.85	2.01	3.41	2.79
Cr_2O_3	–	–	–	–	–	–	–	0.01	bdl	bdl	bdl
Al_2O_3	–	–	–	–	–	–	–	10.12	13.26	10.00	6.75
FeO^T	0.07	0.08	0.05	0.01	0.06	0.76	0.31	24.98	20.18	24.10	23.95
MnO	bdl	0.06	0.02	–	–	–	–	0.89	0.87	0.81	0.64
MgO	–	–	–	0.97	0.52	0.63	0.75	9.45	12.30	10.99	12.18
CaO	54.97	55.09	54.77	53.15	54.67	49.82	51.94	0.08	0.05	bdl	0.02
SrO	0.61	0.63	0.62	0.31	0.14	0.68	0.64	–	–	–	–
BaO	–	–	–	bdl	0.05	0.74	0.60	0.70	0.16	0.23	0.08
Na_2O	0.19	0.17	0.14	0.03	0.02	0.16	0.14	0.49	0.20	0.51	0.43
K_2O	–	–	–	–	–	–	–	8.61	9.57	9.17	9.55
P_2O_5	41.50	41.66	41.98	–	–	–	–	–	–	–	–
La_2O_3	0.06	0.09	0.23	0.02	bdl	0.09	0.04	–	–	–	–
Ce_2O_3	0.23	0.23	0.32	0.03	0.04	0.46	0.38	–	–	–	–
Nd_2O_3	0.18	0.03	0.15	0.01	bdl	0.01	0.02	–	–	–	–
F	4.04	4.15	4.12	–	–	–	–	–	–	–	–
Cl	0.02	0.02	bdl	–	–	–	–	–	–	–	–
O≡F	1.70	1.75	1.74	–	–	–	–	–	–	–	–
O≡Cl	0.00	0.00	0.00	–	–	–	–	–	–	–	–
Total	100.17[a]	100.46[a]	100.67[a]	54.53	55.48	53.36	54.81	96.08	95.38	95.42	94.76
No oxygens	24	24	24	6	6	6	6	22	22	22	22
Si								5.904	5.730	5.773	6.165
Ti								0.464	0.236	0.409	0.337
Cr								0.001	0.000	0.000	0.000
Al								1.910	2.435	1.880	1.277
Fe^{2+}	0.010	0.011	0.007	0.000	0.002	0.023	0.009	3.343	2.629	3.215	3.217
Mn	0.000	0.009	0.003					0.121	0.114	0.109	0.087
Mg				0.049	0.026	0.034	0.039	2.256	2.856	2.614	2.917
Ca	9.841	9.844	9.841	1.943	1.968	1.909	1.924	0.014	0.009	0.000	0.004
Sr	0.059	0.061	0.060	0.006	0.003	0.014	0.013				
Ba				0.000	0.001	0.010	0.008	0.044	0.009	0.015	0.005
Na	0.061	0.054	0.046	0.002	0.001	0.011	0.009	0.153	0.062	0.159	0.134
K								1.758	1.901	1.866	1.957
P	5.871	5.882	5.960								
La	0.004	0.005	0.014	0.000	0.000	0.001	0.001				
Ce	0.014	0.014	0.019	0.000	0.000	0.006	0.005				
Nd	0.011	0.002	0.009	0.000	0.000	0.000	0.000				
Sum cation	15.871	15.882	15.960	2.001	2.000	2.009	2.007	15.969	15.981	16.039	16.099
F	1.067	1.095	1.094								
Cl	0.002	0.003	0.000								
OH calc	0.931	0.902	0.906								

[a] Total minus oxygen for F and Cl; bdl, below detection limit; –, not determined. Mineral abbreviations: ap, apatite; cb, carbonate; mc, mica. OH is calculated assuming (F + Cl + OH) = 2. FeOT, all Fe as FeO.

Table 2
Representative EMP analyses (wt.%) of the major mineral phases of Intrusive carbonatites.

Phase sample	Apatite						Calcite				Biotite	
	CY-116	CY-116	CY-116	CY-145	CY-145	CY-145	CY-116	CY-116	CY-145	CY-1145	CY-116	CY-116
	ap1	ap2	ap8	ap2	ap4	ap7	cb1	cb7	cb2	cb7	mc4	mc8
Major elements (wt.%)												
SiO_2	–	–	–	–	–	–	–	–	–	–	36.12	37.06
TiO_2	–	–	–	–	–	–	0.04	bdl	bdl	bdl	4.41	3.71
Cr_2O_3	–	–	–	–	–	–	–	–	–	–	bdl	0.02
Al_2O_3	–	–	–	–	–	–	–	–	–	–	13.13	12.56
FeOT	0.03	0.07	0.05	0.01	0.02	bdl	0.36	0.30	0.79	0.57	20.16	19.28
MnO	0.04	0.03	0.02	0.02	0.02	0.01	–	–	–	–	0.48	0.45
MgO	–	–	–	–	–	–	0.27	0.27	0.19	0.12	11.54	12.56
CaO	54.69	54.45	55.01	54.41	54.46	54.33	53.64	51.72	52.70	52.37	bdl	0.09
SrO	0.47	0.53	0.55	0.91	0.97	0.88	0.68	0.59	0.15	0.41	-	-
BaO	–	–	–	–	–	–	0.04	0.07	0.02	0.04	0.39	0.30
Na_2O	0.23	0.28	0.24	0.13	0.16	0.16	0.01	0.02	bdl	0.02	0.33	0.33
K_2O	–	–	–	–	–	–	–	–	–	–	9.43	9.50
P_2O_5	42.33	42.20	41.07	42.11	41.91	42.05	–	–	–	–	–	–
La_2O_3	0.03	0.07	0.16	0.15	0.08	0.15	0.01	bdl	0.00	bdl	–	–
Ce_2O_3	0.28	0.39	0.15	0.20	0.26	0.24	0.01	0.07	0.08	0.04	–	–
Nd_2O_3	0.10	0.20	0.07	0.03	0.10	0.05	bdl	bdl	0.018	0.01	–	–
H_2O calc	–	–	–	–	–	–	–	–	–	–	4.01	4.12
F	3.31	3.45	3.64	3.63	3.60	3.51	–	–	–	–	–	–
Cl	0.01	0.01	0.01	bdl	bdl	0.00	–	–	–	–	–	–
O≡F	1.39	1.45	1.53	1.53	1.51	1.48	–	–	–	–	–	–
O≡Cl	0.00	0.00	0.00	–	–	0.00	–	–	–	–	–	–
Total	100.13[a]	100.22[a]	99.42[a]	100.09[a]	100.06[a]	99.90[a]	55.06	53.05	53.95	53.58	95.99	95.88
No oxygens	24	24	24	24	24	24	6	6	6	6	22	22
Si											5.658	5.769
Ti							0.001	0.000	0.000	0.000	0.520	0.434
Cr											0.000	0.003
Al											2.423	2.304
Fe^{2+}	0.004	0.010	0.007	0.001	0.003	0.000	0.010	0.009	0.023	0.017	2.641	2.510
Mn	0.006	0.004	0.002	0.003	0.003	0.002					0.064	0.059
Mg							0.014	0.014	0.010	0.006	2.694	2.921
Ca	9.844	9.802	9.838	9.839	9.821	9.835	1.960	1.962	1.963	1.967	0.000	0.015
Sr	0.046	0.051	0.054	0.089	0.095	0.086	0.013	0.012	0.003	0.008		
Ba							0.000	0.001	0.000	0.001	0.024	0.018
Na	0.075	0.092	0.076	0.044	0.051	0.051	0.001	0.001	0.000	0.001	0.100	0.101
K											1.884	1.887
P	6.021	6.003	5.804	6.017	5.973	6.015						
La	0.002	0.005	0.010	0.009	0.005	0.009	0.000	0.000	0.000	0.000		
Ce	0.017	0.024	0.009	0.012	0.016	0.015	0.000	0.001	0.001	0.001		
Nd	0.006	0.012	0.004	0.002	0.006	0.003	0.000	0.000	0.000	0.000		
Sum cation	16.021	16.003	15.804	16.017	15.973	16.015	2.001	2.001	2.000	2.001	16.008	16.022
F	0.880	0.917	0.960	0.969	0.957	0.938						
Cl	0.001	0.002	0.001	0.000	0.000	0.000						
OH calc	1.119	1.081	1.039	1.031	1.043	1.061						

[a] Total minus oxygen for F and Cl; bdl, below detection limit; –, not determined. Mineral abbreviations: ap, apatite; cb, carbonate; mc, mica. OH is calculated assuming (F + Cl + OH) = 2. FeO^T, all Fe as FeO.

Binder and Troll (1989). As is typical of carbonatite apatites, they are relatively rich in SrO (up to 0.91 wt.%) and poor in MnO (⩽0.06 wt.%). Their light rare earth element contents are clearly higher than those determined for calcite in the same samples, in agreement with the *D* values compiled by Bünh et al. (2001). The rare earth element incorporation was probably accompanied by the incorporation of Na^+ in order to balance charges ($Ca^{2+} + Ca^{2+} \leftrightarrow REE^{3+} + Na^+$; Rønsbo, 1989; Seifert et al., 2000), which would explain the relatively high Na_2O contents (0.13–0.28 wt.%).

In Tables 1 and 2, the calcitic character of carbonates is evident from the low MgO (<0.90 wt.%) and FeO (<0.78 wt.%) contents. Calcites from extrusive carbonatites are clearly more Mg-rich and Fe-poor than their intrusive counterparts, which translates into distinct MgO/(MgO + FeO) contents (extrusives: 0.45–0.99; intrusives: 0.17–0.48). SrO can be as high as 0.69 wt.%.

All present mica is characterised by low X_{phl} (<0.55) and is thus referred to as biotite. K is partially substituted by Na, Ba, and Ca, which occupy up to 11% of the interlayer site. The TiO_2 concentrations are very high (up to 4.41 wt.%), which is remarkable given the very low TiO_2 contents of the host carbonatitic rocks.

5. Whole rock geochemistry

5.1. Analytical procedures

Nineteen samples of extrusive carbonatites considered representative of different outcrops were studied petrographically; of these, nine samples were selected for major and trace element whole rock analyses. The studied samples are representative of two of three areas where extrusive carbonatites were identified (samples CY-219, CY-221, CY-222 and CY-225 come from the north-eastern part of the island, and samples CY-95, CY-231, CY-238, CY-241 and CY-246 were collected in the south). For comparison, data on 12 of 19 collected samples of older intrusive calciocarbonatite were also selected for chemical analysis.

Samples of 1–2 kg were prepared at the Departamento de Geologia da Universidade de Lisboa. After reducing the sample to centimeter-sized chips in a hydraulic press, the freshest pieces were selected and coarsely pound using a jaw crusher and then powdered in an agate swing mill.

Both major- and trace-element analyses were performed at the Activation Laboratories Ltd., Ancaster, Ontario, Canada. For whole rock analysis, major oxide contents were obtained using Inductively Coupled Plasma-Optical Emission Spectrometry (ICP-OES). Trace element contents were obtained using Inductively Coupled Plasma-Mass Spectrometry (ICP-MS), with the exception of Ba and Sr, which were obtained by ICP-OES. Samples were prepared and analysed in a batch system. Each batch contained a method reagent blank, certified reference material and 17% replicates. Samples were mixed with a flux of lithium metaborate and lithium tetraborate and fused in an induction furnace. The molten melt was immediately poured into a solution of 5% nitric acid containing an internal standard and mixed continuously until completely dissolved (~30 min). The samples were run for major oxides and selected trace elements on a combination simultaneous/sequential Thermo Jarrell-Ash ENVIRO II ICP or a Spectro Cirros ICP. Calibration was performed using seven prepared USGS and CANMET certified reference materials. One of the seven standards was used during the analysis for every group of ten samples. The prepared sample solution was spiked with internal standards to cover the entire mass range and was further diluted and introduced into a Perkin Elmer SCIEX ELAN 6000 or 6100 ICP-MS using a proprietary sample introduction methodology. Fluorine was analysed by the Ion Selective Electrode technique (ISE) and CO_2 by Coulometry.

All elements were analysed under the control of certified international standards. In general, there is good agreement between results obtained by different methods on the same samples. Duplicate measurements give an estimate of the total reproducibility of our analyses. For whole rock carbonatite samples, the reproducibility is better than: (i) 1 relative-% for major element contents (SiO_2, Fe_2O_3, MnO, MgO and CaO); (ii) 3 relative-% for Rare Earth Elements; and (iii) 2 relative-% for elements generally highly incompatible in an oceanic context (Rb, Ba, U, Th). The accuracy of the analyses, evaluated by analysing international standards, is generally better than 12 relative-%, with results for many elements within ± 6% of the recommended values. More information on the procedure, precision and accuracy of the Actlabs analyses can be found at http://www.actlabs.com.

Sr and Nd isotope analyses were performed on three representative extrusive calciocarbonatite samples (Upper Unit). Isotopic analyses of two intrusive samples (Middle Unit) were taken from Mata et al. (2006). Whole-rock samples (100 mg) were first treated with distilled water and left at 75 °C for a period of 3 h. After the supernatant were removed, drying of samples at 75 °C on hot plates, dissolution of the residue was performed in Savillex beakers with a mixture of 2 ml HF (45 M) + 0.5 ml HNO_3 (14 M), at 75 °C for 24 h (Savillex closed). Then, 0.2 ml $HClO_4$ (12 M) + 3 ml HNO_3 (7 M) was added to dissolve any residual fluorides. This mixture was evaporated first on a hot plate (at 50 °C for 3 days and 95 °C for 6 h) and then under the *epiradiator* (for 2 h). This was followed by the addition of 5 ml of distilled HCl (6 N) at 75 °C for 24 h and additional drying of the samples at 65 °C on hot plates. The residue was recovered in 10 ml HCl (1.25 M) and centrifuged for 10 min. Sr and Nd separations were performed with the "cascade" column procedure (Sr Spec, True Spec and Ln Spec columns) described by Pin and Bassin (1992) and Pin et al. (1994), after most of the iron was removed through an AG50X4 column. A mixture of HNO_3 (5 M) + HF (0.1 M) was used to collect Sr and REE. Sr and Nd blanks for the complete procedure were <0.5 ng and <0.2 ng, respectively.

Nd and Sr isotope measurements were obtained by thermal ionisation mass spectrometry (TIMS) at the *Laboratoire Magmas et Volcans* (France), using a Finnigan Triton mass spectrometer operating in the static multicollection mode with relay matrix rotation (also called the virtual amplifier) equipped with nine Faraday detectors. Sr samples were loaded on double W filaments with 1 μl H_3PO_4 (3 M) and Nd samples were loaded on the same type of filaments with 1 μl H_3PO_4 (1 M). Measurements of $^{87}Sr/^{86}Sr$ were corrected for ^{87}Rb interference. Sr measurements were mass-fractionation-corrected to $^{86}Sr/^{88}Sr = 0.1194$ and normalised to $^{87}Sr/^{86}Sr = 0.71025$ for the NIST SRM987 standard. Nd isotopic ratios were mass-fractionation-corrected to $^{146}Nd/^{144}Nd = 0.7219$ and normalised to $^{143}Nd/^{144}Nd = 0.51196$ for the Rennes-AMES standard. Repeated analyses of the two standards gave $^{87}Sr/^{86}Sr = 0.710246 \pm 0.000005$ (2σ, $n = 16$) and $^{143}Nd/^{144}Nd = 0.511961 \pm 0.000007$ (2σ, $n = 12$). A typical run consists of at least nine blocks of 10 cycles in order to allow a full rotation of the virtual amplifier system.

5.2. Results

5.2.1. Major and trace elements

Representative major and trace elements compositions of Brava extrusive carbonatites are listed in Table 3. Data on older intrusive calciocarbonatites are also shown for comparison (Table 4).

Independently of the mode of emplacement (pyroclastic deposits vs. lava flows), Brava extrusive carbonatites exhibit a remarkable compositional uniformity, considering that they represent several (at least five) different eruptions and present a wide geographic dispersion. All selected samples of this group yield high CaO contents (>44 wt.%), which classifies them as calciocarbonatite (Fig. 5; Woolley and Kempe, 1989). Despite the fact that their compositional range in terms of $CaO-MgO-Fe_2O_3^t + MnO$ is completely overlapped by the intrusive counterpart, extrusive facies are more iron ($\overline{x}\ Fe_2O_3^t = 6.06$; from 3.31 to 9.76 wt.%) and manganese ($\overline{x}\ MnO = 1.24$; 0.83 to 1.93 wt.%) rich than sövitic rocks ($Fe_2O_3^t:\ \overline{x} = 2.97$; from 0.26 to 13.50 wt.%; $MnO:\ \overline{x} = 0.40$; from 0.23 to 0.87 wt.%).

Extrusive carbonatites are significantly richer in trace elements like Ba, Th, U, Nb, Pb and REE, but somewhat less enriched in Sr than the majority of intrusive calciocarbonatites (Figs. 6 and 7). The latter are compositionally more variable and yield more fractionated REE patterns, with $(La/Yb)_n$ up to 102 vs. up to 35. Both extrusive and intrusive calciocarbonatites are commonly depleted in MREE relative to LREE and HREE, resulting into slightly concave upwards patterns.

Primitive mantle-normalised trace element variations (Fig. 7) show that intrusive calciocarbonatite samples are highly variable, with concentration ranges in some elements of two to three orders of magnitude (e.g., Rb, Th, U, Nb, P and Ti). Significant depletions are observed in K, Th, P, Ti, Zr and Hf, with a few samples yielding abundances below primitive mantle values, which are not uncommon in carbonatites elsewhere (Nelson et al., 1988; Woolley and Kempe, 1989). Fig. 8 further illustrates the chemical differences between intrusive and extrusive carbonatites, as well as the larger variability of the Middle Unit intrusive carbonatites.

5.2.2. Sr–Nd isotopic data

The whole rock Nd and Sr isotopic compositions of Brava calciocarbonatites are listed in Table 6 and plotted in Fig. 9. The element differences reported above are confirmed by isotopic data, which produce two distinct clusters on the $^{143}Nd/^{144}Nd$ vs. $^{87}Sr/^{86}Sr$ diagram. Both groups are characterised by Sr and Nd isotopic signatures indicating their ultimate origin from sources with time-integrated depletion in the more incompatible elements. Intrusive calciocarbonatites of the Middle Unit have higher initial $^{143}Nd/^{144}Nd$ ratios and lower initial $^{87}Sr/^{86}Sr$ ratios than the extrusive calciocarbonatites of the Upper Unit (see Table 6).

Table 3
Major (wt.%) and trace element (ppm) analyses of Extrusive Carbonatites from the Upper Unity of Brava Island.

Sample	Extrusive calciocarbonatites								
	CY-95	CY-219	CY-221	CY-222	CY-225	CY-231	CY-238	CY-241	CY-246
Major elements (wt.%)									
SiO_2	2.03	0.78	1.11	0.56	1.20	3.23	0.85	1.21	1.39
TiO_2	0.183	0.174	0.316	0.198	0.236	0.279	0.166	0.159	0.156
Al_2O_3	0.82	0.23	0.40	0.25	0.40	1.31	0.40	0.38	0.64
$Fe_2O_3^T$	5.06	5.73	9.76	6.38	7.24	7.51	5.04	4.51	3.31
MnO	0.964	1.217	1.929	1.337	1.466	1.464	1.015	0.949	0.832
MgO	1.00	1.12	1.52	1.06	1.16	0.84	0.54	0.72	0.84
CaO	50.04	48.06	48.22	50.96	46.98	44.88	50.04	51.79	49.55
Na_2O	0.20	0.43	0.40	0.21	0.45	0.26	0.13	0.16	0.07
K_2O	0.13	0.03	0.12	0.08	0.09	0.18	0.07	0.13	0.09
P_2O_5	0.90	1.08	2.21	0.98	1.19	1.86	1.09	1.02	0.39
LOI	37.21	37.24	34.08	37.97	36.65	38.12	37.14	37.78	42.44
F	1.10	0.70	0.45	0.46	0.82	1.14	0.77	0.84	0.13
Total	99.64	96.79	100.52	100.45	97.88	101.07	97.25	99.65	99.84
Trace elements (ppm)									
Rb	5.0	4.0	8.0	2.0	7.0	20.0	8.0	12.0	12.0
Sr	6596	7961	6811	4799	8434	7999	6671	5600	3008
Y	157	199	294	193	222	197	159	175	132
Zr	99	108	143	74	113	121	66	68	53
Nb	140	113	186	147	108	102	143	145	75
Cs	0.3	0.1	0.3	<0.1	0.2	2.6	0.2	0.5	0.3
Ba	10330	6019	9200	5634	3834	12140	11460	16130	431
Hf	1.4	2.4	2.5	1.5	2.2	1.8	1.2	1.1	1.0
Ta	0.62	<0.01	<0.01	<0.01	<0.01	<0.01	<0.01	0.51	0.16
Pb	32	38	51	37	44	45	39	34	36
Th	25.3	35.0	56.0	34.4	36.6	35.9	26.7	24.7	20.2
U	4.07	5.24	8.09	2.50	5.67	3.13	3.65	2.47	2.41
La	531	363	722	511	416	421	327	417	506
Ce	507	636	1370	920	725	734	586	759	746
Pr	95	119	170	122	138	136	103	95	89
Nd	311	391	571	405	458	439	341	310	264
Sm	46.4	58.8	87.0	61.5	68.2	66.1	50.5	45.4	34.5
Eu	15.0	18.6	27.8	19.9	22.5	21.3	16.2	15.1	10.9
Gd	38.0	50.0	76.0	54.7	57.0	54.0	41.1	40.3	28.2
Tb	5.11	6.88	10.20	7.15	7.88	7.32	5.50	5.18	3.85
Dy	28.1	36.3	51.5	36.2	41.3	37.8	29.2	28.2	21.2
Ho	5.01	6.62	9.11	6.50	7.26	6.50	5.04	5.48	4.00
Er	13.6	17.9	26.1	17.6	19.5	17.2	13.6	15.9	11.5
Tm	1.81	2.44	3.88	2.44	2.58	2.21	1.75	2.24	1.57
Yb	11.0	15.0	24.2	14.5	15.2	13.0	10.5	13.3	9.7
Lu	1.53	2.10	3.27	1.97	2.06	1.73	1.44	1.79	1.37
∑REE	1609	1724	3152	2180	1980	1957	1532	1754	1732

6. Discussion

6.1. Occurrence and volcano-stratigraphy

On a global scale, extrusive carbonatites are very rare, compared with intrusive ones (Woolley and Church, 2005). Brava extrusive carbonatites are dominated by pyroclastic deposits, which demonstrate that these magmas can be characterised by significant explosivity, despite their extremely low viscosity (see Keller, 1989, for additional examples). Interestingly, one of the Brava occurrences must correspond to a carbonatitic pyroclastic flow deposit, strengthening the conviction that this kind of volcanic events also occurs in carbonatitic volcanism, despite the reservations expressed by Keller (1989).

In Cape Verde, carbonatites are usually assigned to the basal complexes of the islands, being formed during a relatively early stage of the emerged evolution of the volcanic construction (e.g., Serralheiro, 1976; Alves et al., 1979; Silva et al., 1981; Jørgensen and Holm, 2002; Madeira et al., 2005). In Fuerteventura (Canary archipelago), carbonatites are restricted to the basal complex (Muñoz et al., 2005; De Ignacio et al., 2006). Carbonatites on Brava occur in two distinct volcano-stratigraphic positions. Intrusive carbonatites are intimately associated with intrusive plutonic silicate rocks (mainly nepheline syenites, syenites and pyroxenites) belonging to the basal complex, while the extrusive ones correspond to the youngest volcanism of the island. Brava extrusive carbonatites are, therefore, exceptional among the oceanic carbonatites and unique in the context of the Cape Verde geology, as they are associated with the latest magmatic events in the island.

The only age determinations in Brava are those from Obradovich (reported by Lancelot and Allègre (1974)) and Knill (reported by Hoernle et al. (2002)), who measured K–Ar ages of 3.7 and 2.1 Ma, respectively, in biotites of intrusive carbonatites (Middle Unit). Hoernle et al. (2002) suggested for the extrusive carbonatite that they studied an age of <1000 years, based on geomorphological arguments. So far, the ≈2 Ma time lag between the formation of intrusive and extrusive carbonatites cannot be better constrained. However, such a time gap seems reasonable, given that the two episodes of carbonatite formation were separated by a major erosional phase and important uplift of up to 350 m of the submarine formations and intrusive rocks of the basal complex.

6.2. Geochemical comparison with the other Cape Verde carbonatites

In agreement with the time lag mentioned above, the ultimate sources of both groups of Brava carbonatites are clearly distinct, as shown by Sr and Nd isotope differences (Fig. 9). Despite similar

Table 4
Major (wt.%) and trace element (ppm) analyses of Intrusive Carbonatites from the Middle Unit of Brava Island.

Sample	Intrusive calciocarbonatites											
	CY-23	CY-56	CY-116	CY-139	CY-142	CY-144	CY-145	CY-156	CY-157	CY-161	BR-15	BR-23
Major elements (wt.%)												
SiO_2	0.42	0.09	11.92	0.29	2.03	1.49	0.92	5.80	0.36	16.90	3.04	0.27
TiO_2	0.027	<0.001	0.913	<0.001	<0.001	0.621	<0.001	0.049	0.005	0.223	0.216	0.007
Al_2O_3	0.12	0.03	4.37	0.09	0.52	0.33	0.27	0.32	0.19	4.85	0.52	0.10
$Fe_2O_3^T$	0.71	0.26	4.93	1.88	1.38	13.50	0.86	2.79	2.10	4.48	3.93	2.16
MnO	0.500	0.269	0.251	0.528	0.461	0.310	0.352	0.236	0.874	0.233	0.270	0.368
MgO	0.30	0.10	2.31	2.07	0.27	0.13	0.18	0.51	3.80	0.70	0.45	0.12
CaO	53.09	54.64	38.84	51.01	52.11	45.15	52.91	48.48	46.08	37.81	49.75	53.87
Na_2O	0.06	0.04	1.36	0.07	0.32	0.15	0.09	0.89	0.09	2.00	0.31	0.08
K_2O	0.08	<0.01	1.82	<0.01	<0.01	0.12	0.12	0.06	0.05	1.19	0.26	0.05
P_2O_5	0.46	<0.01	4.33	0.37	0.05	1.18	0.12	0.38	0.08	1.67	5.63	0.21
LOI	42.13	43.14	27.23	42.68	41.70	34.93	42.63	38.09	42.31	28.09	34.2	42.33
F	0.08	<0.01	0.55	0.14	0.04	0.12	0.04	0.08	0.23	0.18	-	-
Total	97.98	98.57	98.82	99.13	98.88	98.03	98.49	97.69	96.17	98.33	98.58	99.57
Trace elements (ppm)												
Rb	7.0	<1.0	94.0	<1.0	<1.0	8.0	4.0	9.0	<1.0	38.0	27.0	26.0
Sr	>10000	>10000	5955	3174	7835	8869	8563	>10000	>10000	9152	8466	8622
Y	115	121	117	112	89	93	100	63	145	68	115	99
Zr	<4	<4	160	55	<4	40	<4	316	61	553	103	247
Nb	1.8	0.4	46.6	6.3	2.5	6.0	6.0	4.5	6.5	41.7	10.8	4.6
Cs	<0.1	<0.1	0.9	<0.1	<0.1	<0.1	<0.1	<0.1	<0.1	0.4	-	-
Ba	1016	531	1062	1427	763	454	459	568	5803	1274	314	1041
Hf	0.2	0.2	2.3	0.6	0.2	0.6	0.2	4.2	0.9	8.7	1.5	0.2
Ta	<0.01	<0.01	1.05	<0.01	<0.01	<0.01	0.08	<0.01	<0.01	0.49	-	-
Pb	<5	<5	14	<5	8	6	9	<5	16	6	-	-
Th	0.2	0.1	5.1	28.1	1.9	1.6	10.8	1.0	8.5	6.2	7.1	1.9
U	0.13	0.02	0.71	1.93	1.15	0.49	3.25	0.35	3.60	1.08	1.06	3.11
La	386	354	324	675	285	281	259	196	1380	203	307	280
Ce	671	615	640	1340	496	483	458	314	2560	342	608	502
Pr	66	60	72	133	49	48	45	30	263	34	65	48
Nd	227	209	282	452	163	163	155	98	935	117	241	166
Sm	32.2	30.6	45.8	61.1	24.4	25.6	24.2	14.7	135.0	18.7	39.1	26.8
Eu	10.2	9.5	14.2	16.5	7.3	7.9	7.6	4.5	38.8	5.8	11.1	7.9
Gd	25.8	24.8	36.1	38.1	18.5	20.5	19.6	12.2	92.3	15.3	32.8	22.8
Tb	3.94	3.83	5.21	4.47	2.78	3.13	3.23	1.93	9.82	2.33	4.35	3.33
Dy	21.2	21.0	25.5	21.2	15.2	16.7	17.7	10.4	38.9	12.5	21.5	17.1
Ho	3.96	3.98	4.56	3.87	2.94	3.10	3.36	2.01	6.04	2.32	3.87	3.20
Er	11.5	11.5	11.8	12.5	9.1	8.9	10.2	6.0	14.6	6.7	10.7	9.2
Tm	1.63	1.60	1.49	2.12	1.39	1.26	1.56	0.87	1.69	0.96	1.48	1.36
Yb	10.2	9.7	8.4	16.8	8.9	7.6	10.0	5.1	9.1	5.7	8.4	9.0
Lu	1.47	1.38	1.14	2.77	1.27	1.03	1.39	0.70	1.06	0.80	1.12	1.28
∑REE	1472	1356	1472	2779	1084	1071	1016	697	5485	767	1356	1098

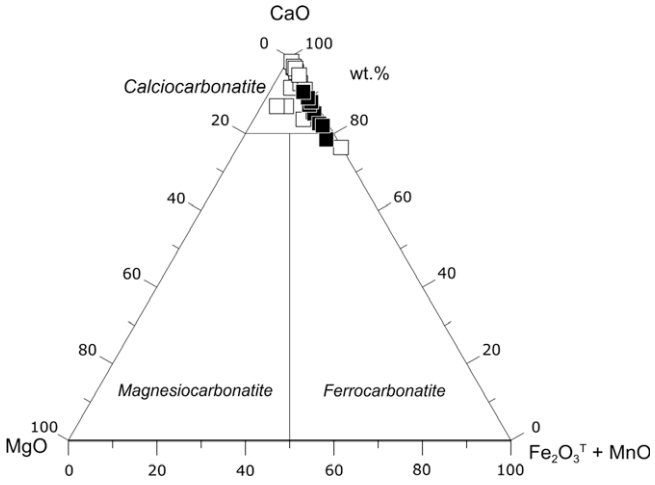

Fig. 5. Extrusive and intrusive carbonatite samples of Brava Island in the classification diagram of Woolley and Kempe (1989) using wt.% oxides. Open squares: intrusive calciocarbonatite, closed squares: extrusive calciocarbonatites.

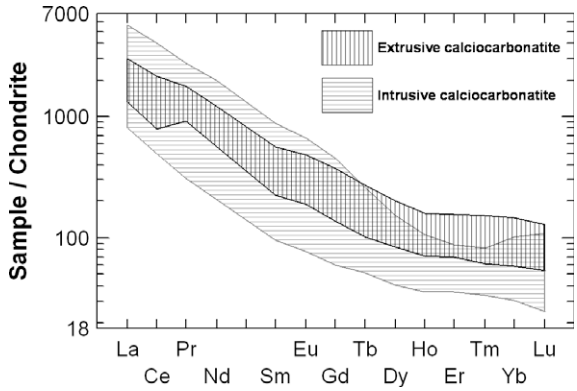

Fig. 6. REE patterns of extrusive calciocarbonatite samples, Upper Unit. Intrusive calciocarbonatites, Middle Unit, are shown for comparison. Normalising values are from Palme and O'Neill (2003).

ranges in isotopic variability, the extrusive carbonatites are clearly more homogeneous than the intrusive ones in terms of their elemental characteristics (Fig. 8), suggesting that they underwent less complex magmatic evolution, like crystal fractionation and/or cumulative processes. This suggests that the extrusive carbonatites were subject to relatively shorter residence times in magma chambers, which, different from occurred for the intrusive magmas, prevented significant magma evolution (see also Woolley and Church,

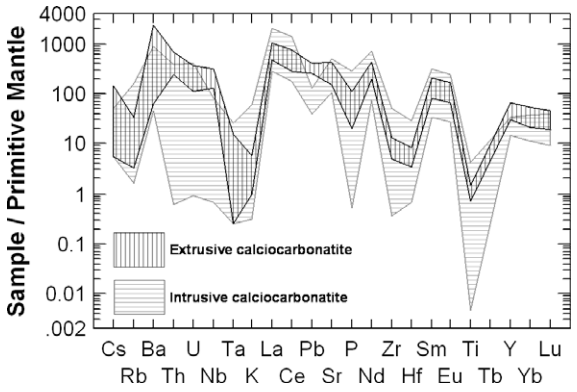

Fig. 7. Trace-element abundances of extrusive calciocarbonatite, Upper Unit, compared with intrusive calciocarbonatite, Middle Unit. Normalising values are from Palme and O'Neill (2003).

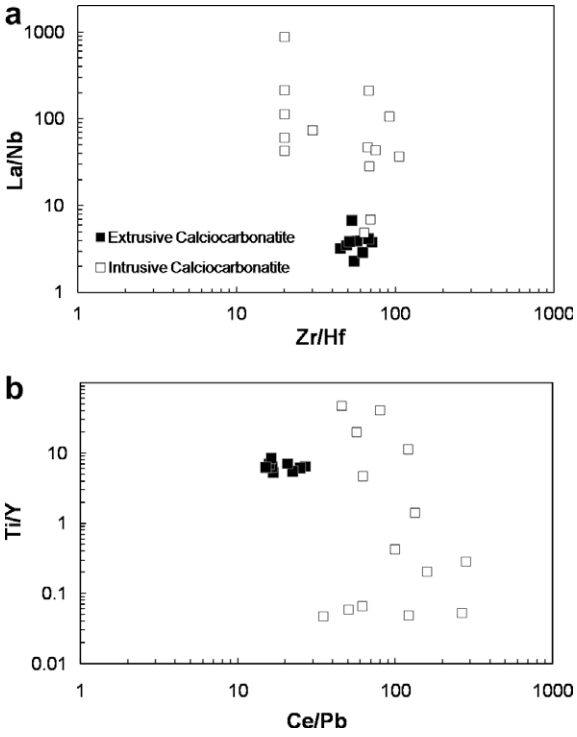

Fig. 8. Zr/Hf vs. La/Nb (a) and Ce/Pb vs. Ti/Y, (b) diagrams comparing extrusive and intrusive calciocarbonatites from Brava Island.

2005). From this perspective, the very pronounced Ti and P negative anomalies of the intrusive carbonatites from the Middle Unit, compared with the extrusive ones, can be explained by the effect of apatite and Ti-rich phase fractionation.

The Cape Verde magmatic rocks are highly heterogeneous in terms of their isotopic signatures. Gerlach et al. (1988) considered that, from an isotopic point of view, the Cape Verde islands can be subdivided into two groups. The northern islands are representative of sources with comparatively higher time-integrated depletion of Rb and Nd relative to Sr and Sm, being simultaneously more radiogenic than the southern islands in terms of $^{206}Pb/^{204}Pb$ ratios (see also Doucelance et al., 2003). The intrusive carbonatites, independent of their occurrence in the northern or southern islands, yield Sr and Nd isotopic compositions that cluster in a zone of the Sr–Nd diagram where the northern and southern silicate rock fields overlap (see Hoernle et al., 2002; Fig. 5). The same conclusion can be drawn from the existing data for Brava intrusive cal-

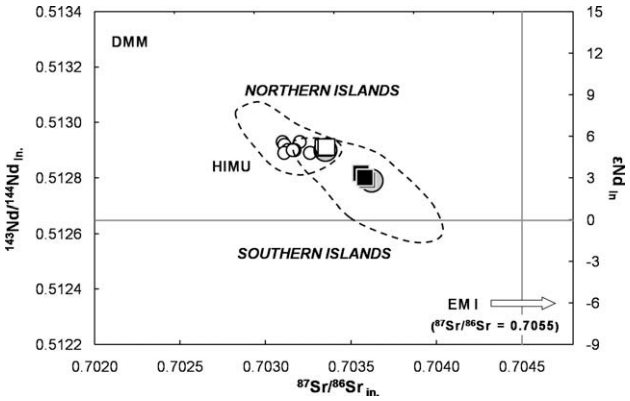

Fig. 9. Initial Nd vs. initial Sr isotope plot. Data are compared with those of other Cape Verde carbonatites: small open circles – Santiago, Fogo and São Vicente calciocarbonatites (Hoernle et al., 2002); large grey-filled circles – Brava calciocarbonatites (intrusive and extrusive occurrences; Hoernle et al., 2002); open squares – Brava intrusive calciocarbonatite (this study); closed squares – Brava extrusive calciocarbonatites (this study). *in*, initial.

ciocarbonatites. However, the extrusive carbonatites described in this paper plot clearly within the field defined by the Southern Cape Verde islands. This demonstrates that the extrusive carbonatites of Brava were ultimately the products of a source clearly distinct from those producing the other Cape Verde carbonatites, either in the northern islands (S. Vicente) or in the southern islands (Maio, Santiago, Fogo and Brava intrusives).

6.3. Petrogenesis

The genesis of carbonatitic magmas is usually addressed in terms of three distinct processes: (1) a very low degree of partial melting of a carbonated peridotite; (2) extreme fractional crystallisation of a carbonated silicate magma; and (3) immiscibility from carbonated nephelinitic or phonolitic magmas (see below for references).

The isotopic similitude between Brava extrusive calciocarbonatites and the silicate rocks from the Upper Unit makes the two last genetic models feasible, whereas in the context of the first hypothesis, it would be possible to hypothesise that the carbonatitic and nephelinitic magmas were ultimately derived from a homogeneous mantle source, with different degrees of partial melting.

Experimental studies on model and natural systems at high pressures (>2.0 GPa) have shown that melting of carbonate-bearing peridotites yields magnesiocarbonatite liquids (e.g., Dalton and Wood, 1993; Wyllie and Lee, 1998; Lee et al., 2000; Foley et al., 2009, and references therein). However, experimental work at lower pressures has shown that magnesiocarbonatite liquids rising through the lithospheric mantle may react with peridotites, forming wehrlites and becoming progressively more calcium-rich as a consequence of the reaction with orthopyroxene to produce olivine and clinopyroxene. If magmas experimentally produced by partial melting process are characterised by Ca/(Ca + Mg) up to 0.88, it is theoretically likely that carbonatitic melts in equilibrium with wehrlite could have Ca/(Ca + Mg) as high as 0.96 (Dalton and Wood, 1993). This is not significantly different from the characteristics of Brava extrusive carbonatites. However, the studied rocks are characterised by very low concentrations in transition elements (Ni < detection limit (20 ppm); Cr < detection limit (5 ppm); Sc < 0.3 ppm) and $Mg/(Mg + Fe^t) < 0.18$, which impede the consideration that the Brava extrusive calciocarbonatites were generated in equilibrium with mantle residual olivine and/or pyroxene (see Eggler, 1989).

Table 5
Major (wt.%) and trace element (ppm) analyses of representative samples of alkaline silicate rocks from the Upper Unit of Brava Island.

Sample	Mafic rocks						Phonolites					
	CY-32	CY-98	CY-124	CY-199	CY-200	CY-247	CY-80	CY-123	CY-168	CY-188	CY-215	CY-265
Major elements (wt.%)												
SiO_2	42.31	39.32	43.88	44.71	44.66	38.81	54.41	51.38	50.80	53.46	46.02	51.91
TiO_2	3.765	3.945	2.839	2.551	2.625	3.836	0.339	0.379	0.353	0.408	2.166	0.394
Al_2O_3	14.39	11.81	15.19	14.97	15.06	11.08	22.20	20.90	21.90	21.79	17.96	21.87
$Fe_2O_3^T$	11.87	12.74	10.33	9.69	9.87	12.70	2.77	3.25	3.39	3.43	8.09	3.41
MnO	0.204	0.205	0.198	0.187	0.188	0.182	0.210	0.136	0.194	0.201	0.201	0.201
MgO	5.76	9.59	6.43	7.47	7.47	12.89	0.13	0.25	0.45	0.23	2.69	0.27
CaO	11.66	13.07	9.74	8.83	8.99	13.09	0.98	1.99	1.68	1.98	7.50	1.76
Na_2O	5.80	3.79	5.53	5.97	5.97	4.47	11.42	11.66	11.26	10.65	9.14	10.03
K_2O	0.92	1.33	2.46	2.88	2.98	2.01	6.33	6.33	6.37	6.34	4.03	7.14
P_2O_5	0.64	0.64	0.56	0.49	0.49	0.55	0.06	0.07	0.04	0.06	0.54	0.05
LOI	1.79	2.65	2.52	1.28	1.02	0.64	1.25	3.73	3.15	2.07	1.41	2.54
Total	99.11	99.08	99.67	99.02	99.33	100.30	100.10	100.10	99.57	100.60	99.75	99.56
Trace elements (ppm)												
Rb	25.0	16.0	36.0	51.0	52.0	42.0	224.0	180.0	210.0	198.0	66.0	224.0
Sr	973	793	998	841	873	726	482	573	747	876	1313	1292
Y	33	31	26	24	26	23	21	13	20	22	31	21
Zr	347	302	342	354	342	214	885	878	733	787	440	725
Nb	87.7	73.7	75.7	74.9	74.5	66.5	128.0	148.0	101.0	111.0	105.0	102.0
Cs	0.9	0.6	1.1	1.1	0.9	0.3	2.6	2.5	2.3	2.6	1.3	2.0
Ba	650	602	1102	877	972	593	254	927	655	1132	1636	1806
Hf	7.8	7.5	7.0	7.4	7.2	5.4	14.6	13.0	10.9	12.2	7.9	10.9
Ta	5.37	5.70	4.34	3.70	3.85	4.09	3.03	4.11	1.77	2.44	4.90	2.30
Pb	8	5	16	7	8	5	22	12	22	22	11	15
Th	6.4	4.7	6.7	7.1	7.0	3.2	17.9	14.4	18.8	18.0	8.9	11.0
U	1.41	1.23	1.63	1.74	1.51	0.84	6.17	4.11	5.86	6.15	1.81	3.27
La	64	55	56	48	50	44	49	31	42	64	80	65
Ce	132	119	114	98	102	93	84	54	72	101	153	110
Pr	14.70	14.00	12.50	10.80	11.20	10.80	7.42	5.30	6.64	9.03	16.20	9.58
Nd	58	57	48	42	44	42	22	18	21	27	56	28
Sm	10.6	10.5	8.7	7.6	7.9	8.3	3.3	2.8	3.3	3.9	9.3	4.1
Eu	3.5	3.5	2.9	2.5	2.7	2.7	1.1	0.9	1.1	1.3	3.1	1.3
Gd	9.9	10.1	7.8	7.0	7.3	7.1	2.6	2.2	2.4	2.8	7.3	3.2
Tb	1.38	1.32	1.11	1.00	1.03	1.00	0.50	0.37	0.48	0.53	1.11	0.57
Dy	6.84	6.39	5.69	5.00	5.25	5.05	3.12	2.18	3.08	3.36	5.72	3.41
Ho	1.18	1.13	0.99	0.89	0.94	0.83	0.66	0.43	0.64	0.71	1.03	0.68
Er	3.06	2.91	2.59	2.37	2.44	2.10	2.23	1.31	2.09	2.32	2.80	2.12
Tm	0.421	0.384	0.353	0.330	0.344	0.255	0.385	0.211	0.349	0.387	0.391	0.341
Yb	2.43	2.21	2.09	2.04	2.08	1.44	2.64	1.45	2.51	2.70	2.41	2.36
Lu	0.333	0.297	0.298	0.286	0.290	0.189	0.413	0.217	0.385	0.421	0.339	0.348
∑REE	309	284	263	227	237	219	180	120	158	220	338	231

Table 6
Strontium and neodymium isotopic compositions of Brava carbonatites.

Sample	Occurrence	Type	Age (Ma)	[Rb] (ppm)	[Sr] (ppm)	$^{87}Rb/^{86}Sr$	$^{87}Sr/^{86}Sr$		[Sm] (ppm)	[Nd] (ppm)	$^{147}Sm/^{144}Nd$	$^{143}Nd/^{144}Nd$	
							Measured	Initial				Measured	Initial
BR-15[a]	Intrusive	Ca-carb.	2	27	8466	0.0092	0.703340 (12)	0.703340	39.1	241	0.0981	0.512910 (07)	0.512908
BR-23[a]	Intrusive	Ca-carb.	2	1	8622	0.0003	0.703356 (08)	0.703356	26.8	166	0.0976	0.512912 (09)	0.512911
CY-95	Extrusive	Ca-carb.	0	5	6596	0.0022	0.703595 (06)	0.703595	46.4	311	0.0902	0.512792 (05)	0.512792
CY-222	Extrusive	Ca-carb.	0	2	4799	0.0012	0.703557 (07)	0.703557	61.5	405	0.0918	0.512816 (08)	0.512816
CY-238	Extrusive	Ca-carb.	0	8	6671	0.0035	0.703580 (06)	0.703580	50.5	341	0.0895	0.512801 (06)	0.512801

[a] Isotopic analysis were taken from Mata et al. (2006).

Petrological evidence for the formation of carbonatite magma through extreme fractionation of a carbonated silicate parent has been presented by some authors (e.g., Watkinson and Wyllie, 1971; Otto and Wyllie, 1993; Lee and Wyllie, 1994; Church and Jones, 1995). This implies that variation diagrams are characterised by discernible liquid-line-of-descent that can explain the evolution, by fractional crystallisation, from silicate to carbonatitic magmas. Clearly, this is not observed for volcanics of the Upper Unit (Table 5, Fig. 10). Indeed, the Zr depletion of carbonatites cannot be explained by fractionation of zircon or amphibole, because this would also deplete carbonatitic magmas in Lu and Th, in the case of zircon, and in Y in the case of amphibole, which is not observed. Moreover, none of these mineral phases are reported in the phonolitic rocks. In addition, the significant K_2O depletion of carbonatites cannot be explained by alkali feldspar fractionation, given the carbonatite enrichment in Sr and Ba relative to phonolites (Fig. 10).

The frequent intimate association of carbonatites with highly silica-undersaturated, alkaline, silicate rocks, coupled with field and melt inclusion evidence, gave rise to the hypothesis that carbonatitic magmas could be generated through liquid immiscibility, an idea repeatedly confirmed by experimental data (e.g., Koster van Groos and Wyllie, 1963; Kjarsgaard and Hamilton, 1988, 1989; Kjarsgaard and Peterson, 1991; Kjarsgaard et al., 1995; Lee and Wyllie, 1997, 1998a, 1998b; Ray and Shukla, 2004; Panina and Motorina, 2008). It has been suggested that pure calciocarbonatites (>80% $CaCO_3$) cannot form by immiscibility and must be

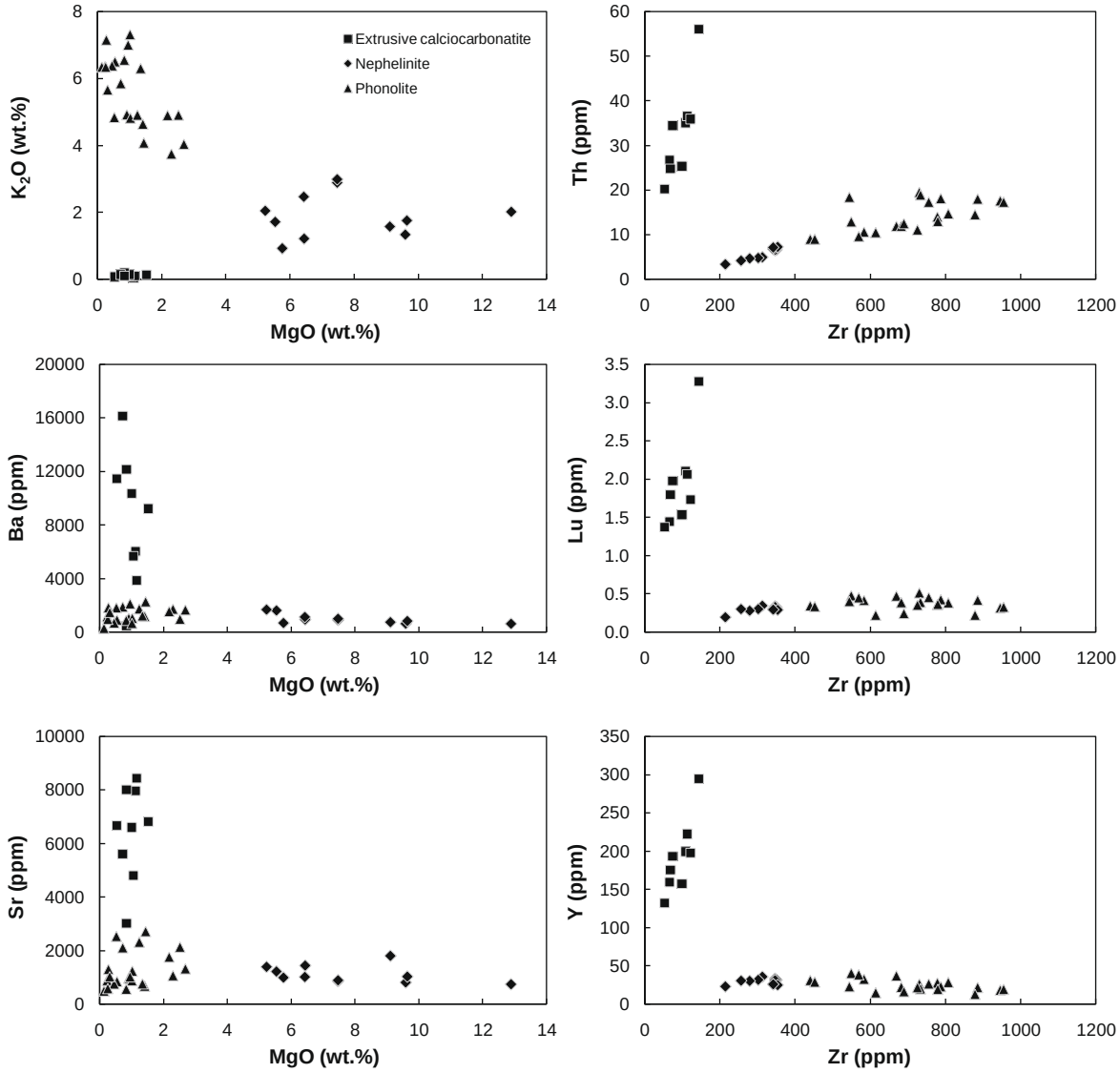

Fig. 10. Plot of K_2O, Ba and Sr vs. MgO, and Th, Lu and Y vs. Zr for alkaline silicate rocks and extrusive calciocarbonatites from Brava.

considered cumulates, given that they plot in the so-called "forbidden volume" in $[CaO + MgO - FeO^t]$–$[Na_2O + K_2O]$–$[SiO_2 + Al_2O_3 + TiO_2]$-space (Lee and Wyllie, 1996). From this perspective, Brava extrusive carbonatites and most of the naturally occurring calciocarbonatites cannot represent the carbonate fraction that was separated by immiscibility from a silicate parent. However, Kjarsgaard (1998) obtained calciocarbonatite liquids with very high Ca/(Ca + Mg) ratios (down to 0.91) and moderate alkali contents through low-pressure (0.2–0.5 GPa) liquid immiscibility experiments, providing support for the possibility of a genesis of calciocarbonatites by immiscibility. In order to test the applicability of the immiscibility model for the Brava extrusive calciocarbonatites, their compositions and those from their potential silicate conjugates (Table 5) were plotted on the pseudo-ternary triangle $(SiO_2 + Al_2O_3)$–$(Na_2O + K_2O)$–Cafemics presented by Freestone and Hamilton (1980) (Fig. 11). From the positioning in this diagram, carbonatites can be viewed as the result of an immiscibility process, from which also resulted a silicate conjugate of nephelinitic composition, given that they plot at the opposite ends of one of the experimental conjugation lines. If this model applies to the studied rocks, the trace-element enrichment/depletion of the extrusive calciocarbonatites with respect to their potential silicate conjugates should be consistent with the available experimental data on the trace-element partitioning between immiscible silicate–carbonate liquids. Fig. 12 shows the concentrations of selected elements of three extrusive carbonatites, normalised to the composition of the nephelinitic rock from the Upper Unit (Table 5) plotting closest to the solvus and to the end of the conjugation line.

With respect to the nephelinitic rock, the calciocarbonatites are highly depleted in the alkaline elements K, Na, Rb and Cs, and also in Zr, Hf, Ta and Ti. However, they are enriched in P, Sr, Ba, Nb and REE. These results are in agreement with the experimental data obtained by Veksler et al. (1998) for the partitioning of trace elements between carbonatitic and silicate melts: $D_{Ba}^{carb/sil} = 5.2$; $D_{Sr}^{carb/sil} = 4.1$; $D_{Ti}^{carb/sil} = 0.41$; $D_{Zr}^{carb/sil} = 0.016$; $D_{Nb}^{carb/sil} = 0.503$; $D_{Ta}^{carb/sil} = 0.099$. Note that this process also offers a plausible explanation for the decoupling between pairs of elements considered geochemically coherent. Indeed, the Nb/Ta and Zr/Hf ratios of carbonatitic and nephelinitic rocks are clearly distinct (carbonatites: Nb/Ta $\geqslant$ 226, Zr/Hf $\geqslant$ 45; nephelinites: Nb/Ta $\leqslant$ 16.3, Zr/Hf $\leqslant$ 42.3), reflecting significant differences in the partition coefficients of these elements during immiscibility $K_{D\,Nb/Ta}^{carb/sil} = 5.1$; $K_{D\,Zr/Hf}^{carb/sil} = 1.7$; Veksler et al., 1998). In conclusion, the isotopic similarity between carbonatites and contemporaneous nephelinitic rocks, their positioning in the $(SiO_2 + Al_2O_3)$–$(Na_2O + K_2O)$–Cafemics diagram, and the

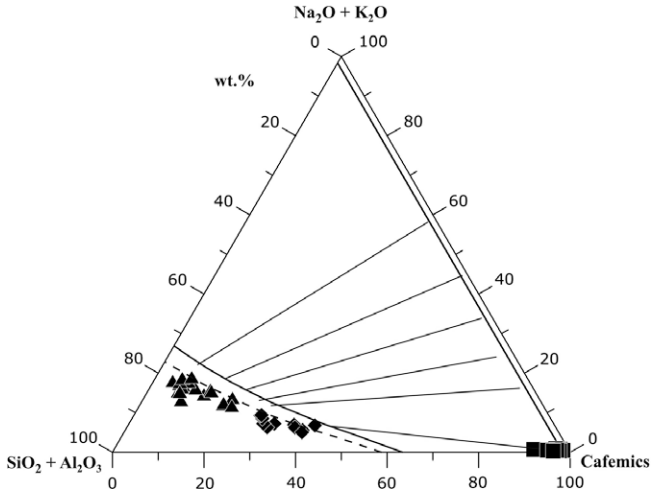

Fig. 11. Carbonate–silicate liquid immiscibility in the experimental system ($SiO_2 + Al_2O_3$)–($Na_2O + K_2O$)–Cafemics (CaO + FeO + MgO + MnO) (Kjarsgaard and Hamilton, 1988). The silicate limb of immiscibility at 0.5 GPa (bold continuous line) and 0.8 GPa (dashed line) and experimentally determined tie-lines to different carbonatite compositions are indicated. Symbols are the same as those used in Fig. 10. Our alkaline silicate rocks present an evolution along the limb of the solvus for 0.8 GPa. The compositions of some nephelinites found in association with the carbonatites can be seen to have conjugate liquids carbonates plotting very close to the Cafemic corner, i.e., very poor in K + Na, but rich in Ca, Mg, Fe, Mn.

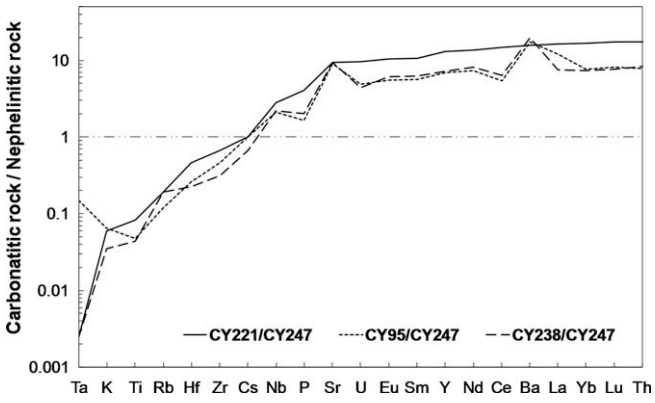

Fig. 12. Enrichment factor for selected elements of three extrusive calciocarbonatites with respect to the composition of a nephelinitic rock from the Upper Unit (sample CY-247) plotting closest to the solvus and to the end of the conjugation line drawn in Fig. 11.

elemental characteristics of these two types of rocks support a carbonatite genesis by carbonate/silicate liquid unmixing. This genetic model is also supported by the close temporal and spatial association of carbonatites and nephelinites.

Hamilton et al. (1989) demonstrated a significant pressure dependence of the $D^{sil/carb}$ for the rare earth elements. The $D^{sil/carb}$ values for REE decrease as P increases, becoming slightly less than 1 at about 0.6 GPa. This means that the REE enrichment of Brava carbonatites relative to nephelinites points to the occurrence of the immiscibility process at pressures of at least around 0.6 GPa.

The occurrence of immiscibility processes in the Upper Unit of Brava was already suggested by Kogarko (1993), who described the occurrence of carbonatite globules in phonolitic rocks. However, from our data we conclude that phonolite–carbonatite melt unmixing was not responsible for the generation of the outcropping carbonatites. Indeed, these are too alkali-poor to have been in equilibrium with melts of phonolitic composition (Fig. 11).

7. Conclusions

On the Island of Brava (Cape Verde), carbonatites occur in two distinct volcano-stratigraphic positions. Intrusive carbonatites are intimately associated with intrusive plutonic silicate rocks (mainly nepheline syenites, syenites and pyroxenites) belonging to the basal complex, whereas extrusive ones, the central aim of this paper, are part of the youngest volcanism of the island.

At least 20 small outcrops of dark-brown to blackish extrusive carbonatites were found on this island, most of which were made up of pyroclastic products, comprising magmatic and/or phreatomagmatic ash and lapilli fall deposits and one probable pyroclastic flow. Lava (alvikite) flows may also be present in one locality (Santa Bárbara). These extrusive carbonatites, corresponding to at least five distinct eruptions, are unique in the context of the Cape Verde geology, given that they are the only ones formed during a late stage of the development of island building. They are also unique in terms of geochemistry. Indeed, extrusive carbonatites have lower $^{143}Nd/^{144}Nd$ and higher $^{87}Sr/^{86}Sr$ compared with all other Cape Verde carbonatites, either in the northern (S. Vicente) or in the southern islands (Maio, Santiago, Fogo and Brava intrusives), plotting clearly within the field defined by the silicate rocks of the Southern group of Cape Verde.

Based on the results obtained in this study for carbonatites and silicate rocks from Brava, we propose a genetic model invoking carbonatite–nephelinite immiscibility. This is supported by the intimate association of carbonatites with nephelinitic rocks, the similarities in their radiogenic isotope signatures, the comparison of their major element compositions with the results of experimental data, and carbonatite/nephelinite trace element enrichment/depletion factors compatible with experimental data on the partitioning of trace elements between nephelinite/carbonate liquid pairs.

Acknowledgements

This work was supported by FCT/FEDER through project PLINT (POCTI/CTA/45802/2002), GEODYN (LATTEX, POCTI-ISFL-5-32) and by a PhD scholarship from FCT (SFRH/BD/39493/2007) co-financed by FEDER for C. Mourão. We also acknowledge the supports of the Calouste Gulbenkian Fundation, which provided access to the analytical facilities of the Institute de Physique du Globe de Paris and the Laboratoire Magmas et Volcans (France). The authors are grateful to C. Bosq and P. Rodrigues for skilled assistance during the chemical separation of Sr and Nd and electron microprobe analyses, respectively. We acknowledge the suggestions of the reviewers Bernard Bonin and Christian Koeberl, which helped to improve this paper.

References

Aires-Barros, L., 1968. Petrografia do ilhéu Grande (ilha Brava, Cabo Verde). Garcia de Orta 16, 249–258.

Allègre, C.J., Pineau, F., Bernat, M., Javoy, M., 1971. Evidence for the occurrence of carbonatites on Cape Verde and Canary Islands. Nature Physical Science 233, 103–104.

Alves, M.C.A., Macedo, J.R., Silva, L.C., Serralheiro, A., Peixoto Faria, A.F., 1979. Estudo geológico, petrológico e vulcanológico da ilha de Santiago (Cabo Verde). Garcia de Orta 3 (1–2), 47–74.

Assunção, C.F.T., Machado, F., Gomes, R.A.D., 1965. On the occurrence of carbonatites in the Cape Verde Islands. Boletim da Sociedade Geológica de Portugal 16, 179–188.

Bailey, D.K., 1993. Carbonate magmas. Journal of the Geological Society 150, 637–651.

Binder, G., Troll, G., 1989. Coupled anion substitution in natural carbon-bearing apatites. Contributions to Mineralogy and Petrology 101, 394–401.

Brassinnes, S., Balaganskaya, E., Demaiffe, D., 2005. Magmatic evolution of the differentiated ultramafic, alkaline and carbonatite intrusion of Vuoriyarvi (Kola Peninsula, Russia).A LA-ICP-MS study of apatite. Lithos 85, 76–92.

Bünh, B., Wall, F., Le Bas, M.J., 2001. Rare-earth element systematics of carbonatitic fluorapatites, and their significance for carbonatite magma evolution. Contributions to Mineralogy and Petrology 141, 572–591.

Chauvel, C., McDonough, W., Guille, G., Maury, R., Duncan, R., 1997. Contrasting old and young volcanism in Rurutu Island, Austral chain. Chemical Geology 139, 125–143.

Church, A.A., Jones, A.P., 1995. Silicate–carbonate immiscibility at Oldoinyo Lengai. Journal of Petrology 36, 869–889.

Coltorti, M., Bonadiman, C., Hinton, R.W., Siena, F., Upton, B.G.J., 1999. Carbonatite metasomatism of the oceanic upper mantle: evidence from clinopyroxenes and glasses in ultramafic xenoliths of Grande Comore, Indian Ocean. Journal of Petrology 40, 133–165.

Dalton, J.A., Wood, B.J., 1993. The compositions of primary carbonate melts and their evolution through wallrock reaction in the mantle. Earth and Planetary Science Letters 119, 511–525.

De Ignacio, C., Muñoz, M., Sagredo, J., Fernández-Santín, S., Johansson, A., 2006. Isotope geochemistry and FOZO mantle component of the alkaline–carbonatitic association of Fuerteventura, Canary Islands, Spain. Chemical Geology 232, 99–113.

D'Orazio, M., Innocenti, F., Tonarini, S., Doglioni, C., 2007. Carbonatites in a subduction system: The Pleistocene alvikites from Mt. Vulture (southern Italy). Lithos 98, 313–334.

Doucelance, R., Escrig, S., Moreira, M., Gariépy, C., Kurz, M.D., 2003. Pb–Sr–He isotope and trace element geochemistry of the Cape Verde Archipelago. Geochimica et Cosmochimica Acta 67, 3717–3733.

Eggler, D.H., 1989. Carbonatites, primary melts and mantle dynamics. In: Bell, K. (Ed.), Carbonatites – Genesis and Evolution. Unwin Hyman, London, pp. 561–579.

Foley, S.F., Yaxley, G.M., Rosenthal, A., Buhre, S., Kiseeva, E.S., Rapp, R.P., Jacob, D.E., 2009. The composition of near-solidus melts of peridotite in the presence of CO_2 and H_2O between 40 and 60 kbar. Lithos, doi:10.1016/j.lithos.2009.03.020.

Freestone, I.C., Hamilton, D.L., 1980. The role of liquid immiscibility in the genesis of carbonatites – an experimental study. Contributions to Mineralogy and Petrology 73, 105–117.

Fúster, J.M., Cendrero, A., Gastesi, P., Ibarrola, E., López-Ruiz, J., 1968. Geología y Volcanología de las Islas Canarias, Fuerteventura. Instituto Lucas Mallada, CSIC, Madrid. 239 p.

Gerlach, D.C., Cliff, R.A., Davies, G.R., Norry, M., Hodgeson, N., 1988. Magma sources of the Cape Verdes Archipelago: isotopic and trace element constraints. Geochimica et Cosmochimica Acta 52, 2979–2992.

Hamilton, D.L., Bedson, P., Esson, J., 1989. The behavior of trace elements in the evolution of carbonatites. In: Bell, K. (Ed.), Carbonatites: Genesis and Evolution. Unwin Hyman, London, pp. 405–427.

Hauri, E.H., Shimizu, N., Dieu, J.J., Hart, S.R., 1993. Evidence for hotspot-related carbonatite metasomatism in the oceanic upper mantle. Nature 364, 221–227.

Hoernle, K.A., Tilton, G., LeBas, M.J., Duggen, S., Garbe-Schönberg, D., 2002. Geochemistry of oceanic carbonatites compared with continental carbonatites: mantle recycling of oceanic crustal carbonate. Contributions to Mineralogy and Petrology 142, 520–542.

Jørgensen, J.Ø., Holm, P.M., 2002. Temporal variation and carbonatite contamination in primitive ocean island volcanics from Sao Vicente, Cape Verde Islands. Chemical Geology 192, 249–267.

Keller, J., 1989. Extrusive carbonatites and their significance. In: Bell, K. (Ed.), Carbonatites: Genesis and Evolution. Unwin Hyman, London, pp. 70–88.

Kjarsgaard, B.A., 1998. Phase relations of a carbonated high-CaO nephelinite at 0.2 and 0.5 GPa. Journal of Petrology 39, 2061–2075.

Kjarsgaard, B.A., Hamilton, D.L., 1988. Liquid immiscibility and the origin of alkali-poor carbonatites. Mineralogical Magazine 52, 43–55.

Kjarsgaard, B.A., Hamilton, D.L., 1989. The genesis of carbonatites by immiscibility. In: Bell, K. (Ed.), Carbonatites: Genesis and Evolution. Unwin Hyman, London, pp. 388–404.

Kjarsgaard, B.A., Peterson, T.D., 1991. Nephelinite–carbonatite immiscibility at Shombole volcano, East Africa: petrographic and experimental evidence. Mineralogy and Petrology 43, 293–314.

Kjarsgaard, B.A., Hamilton, D.L., Peterson, T.D., 1995. Peralkaline nephelinite/carbonatite liquid immiscibility: comparison of phase compositions in experiments and natural lavas from Oldoinyo Lengai. In: Bell, K., Keller, J. (Eds.), Carbonatite Volcanism: Oldoinyo Lengai and the Petrogenesis of Natrocarbonatites. Springer-Verlag, Berlin, pp. 4–22.

Kogarko, L.N., 1993. Geochemical characteristics of oceanic carbonatites from the Cape Verde Islands. South African Journal of Geology 96, 119–125.

Koster van Groos, A.F., Wyllie, P.J., 1963. Experimental data bearing on the role of liquid immiscibility in the genesis of carbonatites. Nature 199, 801–802.

Lancelot, J.R., Allègre, C.J., 1974. Origin of carbonatite magma in the light of the Pb–U–Th isotope system. Earth and Planetary Science Letters 22, 233–238.

Lee, W.-J., Wyllie, P.J., 1994. Experimental data bearing on liquid immiscibility, crystal fractionation, and the origin of calciocarbonatites. International Geology Review 36, 797–819.

Lee, W.J., Wyllie, P.J., 1996. Liquid immiscibility in the join $NaAlSi_3O_8$-$CaCO_3$ to 2.5 GPa and the origin of calciocarbonatite magmas. Journal of Petrology 37, 1125–1152.

Lee, W.-J., Wyllie, P.J., 1997. Liquid immiscibility in the join $NaAlSiO_4$–$NaAlSi_3O_8$ $CaCO_3$ at 1 GPa: Implications for crustal carbonatites. Journal of Petrology 38, 1113–1135.

Lee, W.-J., Wyllie, P.J., 1998a. Petrogenesis of Carbonatite Magmas from Mantle to Crust, Constrained by the System CaO–(MgO + FeO)–(Na_2O + K_2O)–(SiO_2 + Al_2O_3 + TiO_2)–CO_2. Journal of Petrology 37, 495–517.

Lee, W.-J., Wyllie, P.J., 1998b. Processes of crustal carbonatite formation by liquid immiscibility and differentiation, elucidated by model systems. Journal of Petrology 39, 2005–2013.

Lee, W.-J., Fanelli, M.F., Cava, N., Wyllie, P.J., 2000. Calciocarbonatite and magnesiocarbonatite rocks and magmas represented in the system CaO–MgO–CO2–H2O at 0.2 GPa. Mineralogy and Petrology 68, 225–256.

Machado, F., Azeredo Leme, J., Monjardino, J., Seita, M.F., 1968. Carta geológica de Cabo Verde, notícia explicativa da Ilha Brava e dos Ilhéus Secos. Garcia de Orta 16, 123–130.

Madeira, J., Munhá, J., Tassinari, C.C.G., Mata, J., Brum da Silveira, A., Martins, S., 2005. K/Ar Ages of Carbonatites from the Island of Fogo (Cape Verde). XIV Semana de Geoquímica/VIII Congresso de Geoquímica dos Países de Língua Portuguesa. Aveiro, Portugal. pp. 475–478.

Madeira, J., Mata, J., Mourão, C., 2006. Volcano-tectonic structure of Brava Island (Cape Verde). VII Congresso Nacional de Geologia. Évora, Portugal. pp. 279–282.

Madeira, J., Brum da Silveira, A., Mata, J., Mourão, C., Martins, S., 2009. The role of mass movements on the geomorphologic evolution of island volcanoes: examples from Fogo and Brava in the Cape Verde archipelago. Comunicações Geológicas 95, 99–112.

Martins, S., Mata, J., Munhá, J., Mattielli, N., 2007. Plume–lithosphere interaction at Santiago Island (Cape Verde) (abstract). Geochimica et Cosmochimica Acta 75 (15S), A630.

Mata, J., Munhá, J., Kerrich, R., 1999. Evidências para a ocorrência de metassomatismo carbonatítico na fonte mantélica da Ilha da Madeira (abstract). In: Anais do V Congresso Geoquímico dos Países de Língua Portuguesa Porto Seguro, Brasil. pp. 550–551.

Mata, J., Moreira, M., Doucelance, R., Silva, L.C., Martins, S., Mourão, C., Raquin, A., Martins, L., Madureira, P., 2006. Sr, Nd and noble gases isotopic constraints on the origin of the Cape Verde carbonatites (abstract). VII Congresso Nacional de Geologia. Évora, Portugal. pp. 201–203.

Mattielli, N., Weis, D., Blichert-toft, J., Albarede, F., 2002. Hf isotope evidence for a Miocene change in the Kerguelen Mantle plume composition. Journal of Petrology 43, 1327–1339.

Monnereau, M., Cazenave, A., 1990. Depth and geoid anomalies over oceanic hotspot swells: a global survey. Journal of Geophysical Research 95, 429–438.

Montelli, R., Nolet, G., Dahlen, F.A., Masters, G., 2006. A catalogue of deep mantle plumes: new results from finite-frequency tomography. Geochemistry, Geophysics, Geosystems 7, Q11007. doi:10.1029/2006GC001248.

Muñoz, M., Sagredo, J., de Ignacio, C., Fernández-Suárez, J., Jeffries, T.E., 2005. New data (U–Pb, K–Ar) on the geochronology of the alkaline–carbonatitic association of Fuerteventura, Canary Islands, Spain. Lithos 85, 140–153.

Nelson, D.R., Chivas, A.R., Chappell, B.W., McCulloch, M.T., 1988. Geochemical and isotopic systematics in carbonatites and implications for the evolution of ocean island sources. Geochimica et Cosmochimica Acta 52, 1–17.

Otto, J.W., Wyllie, P.J., 1993. Relationships between silicate melts and carbonate-precipitating melts in CaO–MgO–SiO2–CO2–H2O at 2 kbar. Mineralogy and Petrology 48, 343–365.

Palme, H., O'Neill, H., 2003. Cosmochemical estimates of mantle compositions. In: Carlson, R. (Ed.), Treatise on Geochemistry. The Mantle and Core, vol. 2. Elsevier, Washington, pp. 1–38.

Panina, L.I., Motorina, I.V., 2008. Liquid immiscibility in deep-seated magmas and the generation of carbonatite melts. Geochemistry International 46, 448–464.

Peterson, A.L., Wolff, J.A., Turbeville, B.N., 1989. Eruption mechanisms of extrusive carbonatites on an ocean island: Brava, Cape Verde islands. EOS Transactions of the American Geophysical Union 70, 1421 (abstract).

Pin, C., Bassin, C., 1992. Evaluation of a strontium-specific extraction chromatographic method for isotopic analysis in geological materials. Analytica Chimica Acta 269, 249–255.

Pin, C., Briot, D., Bassin, C., Poitrasson, F., 1994. Concomitant separation of strontium and samarium–neodymium for isotopic analysis in silicate samples, based on specific extraction chromatography. Analytica Chimica Acta 268, 209–217.

Ray, J., Shukla, P.N., 2004. Trace element geochemistry of Amba Dongar carbonatite complex, India: Evidence for fractional crystallization and silicate–carbonate melt immiscibility. Proceedings – Indian Academy of Science 113, 519–531.

Rønsbo, J.G., 1989. Coupled substitutions involving REEs and Na and Si in apatites in alkaline rocks from the Ilimaussaq intrusion, South Greenland. American Mineralogist 74, 896–901.

Seifert, W., Kämpf, H., Wasternack, J., 2000. Compositional variation in apatite, phlogopite and other accessory minerals of the ultramafic Delitzsch complex, Germany: implication for cooling history of carbonatites. Lithos 53, 81–100.

Serralheiro A., 1976. A geologia da ilha de Santiago. Boletim do Museu e Laboratório Mineralógico e Geológico da Faculdade de Ciências de Lisboa, vol. 14, 218 p.

Silva, L., Le Bas, M.J., Robertson, A.H.F., 1981. An oceanic carbonatite volcano on Santiago, Cape Verde Islands. Nature 294, 644–645.

Veksler, I.V., Petibon, C., Jenner, G.A., Dorfman, A.M., Dingwell, D.B., 1998. Trace element partitioning in immiscible silicate–carbonate liquid systems: an initial experimental study using a centrifuge autoclave. Journal of Petrology 39, 2095–2104.

Watkinson, D.H., Wyllie, P.J., 1971. Experimental study of the join NaAlSi3O8-CaCO3–H2O and the genesis of alkalic rock carbonatite complexes. Journal of Petrology 12, 357–378.

Woolley, A.R., Church, A.A., 2005. Extrusive carbonatites: a brief review. Lithos 85, 1–14.

Woolley, A.R., Kempe, D.R.C., 1989. Carbonatites: nomenclature, average chemical compositions, and element distribution. In: Bell, K. (Ed.), Carbonatites: Genesis and Evolution. Unwin Hyman, London, pp. 1–14.

Wyllie, P.J., Lee, W.-J., 1998. Model system controls on conditions for formation of magnesiocarbonatite and calciocarbonatite magmas from the mantle. Journal of Petrology 39, 1885–1893.